The EMBO Journal (2012) 31, 4404–4414 | © 2012 European Molecular Biology Organization | All Rights Reserved 0261-4189/12
www.embojournal.org

THE EMBO JOURNAL

TNFα signals through specialized factories where responsive coding and miRNA genes are transcribed

Argyris Papantonis[1,7], Takahide Kohro[2,7], Sabyasachi Baboo[1], Joshua D Larkin[1], Binwei Deng[1], Patrick Short[1,3], Shuichi Tsutsumi[4], Stephen Taylor[5], Yasuharu Kanki[4], Mika Kobayashi[4], Guoliang Li[6], Huay-Mei Poh[6], Xiaoan Ruan[6], Hiroyuki Aburatani[4], Yijun Ruan[6], Tatsuhiko Kodama[4], Youichiro Wada[4,*] and Peter R Cook[1,*]

[1]The Sir William Dunn School of Pathology, University of Oxford, Oxford, UK, [2]Department of Translational Research for Healthcare and Clinical Science, Graduate School of Medicine, University of Tokyo, Tokyo, Japan, [3]Department of Applied Mathematics and Quantitative Biology, University of North Carolina, Chapel Hill, NC, USA, [4]Laboratory for Systems Biology and Medicine, Research Center for Advanced Science and Technology, University of Tokyo, Tokyo, Japan, [5]Computational Research Biology Group, University of Oxford, Oxford, UK and [6]Genome Institute of Singapore, Singapore, Singapore

Tumour necrosis factor alpha (TNFα) is a potent cytokine that signals through nuclear factor kappa B (NFκB) to activate a subset of human genes. It is usually assumed that this involves RNA polymerases transcribing responsive genes wherever they might be in the nucleus. Using primary human endothelial cells, variants of chromosome conformation capture (including 4C and chromatin interaction analysis with paired-end tag sequencing), and fluorescence *in situ* hybridization to detect single nascent transcripts, we show that TNFα induces responsive genes to congregate in discrete 'NFκB factories'. Some factories further specialize in transcribing responsive genes encoding micro-RNAs that target downregulated mRNAs. We expect all signalling pathways to contain this extra leg, where responding genes are transcribed in analogous specialized factories.

The EMBO Journal (2012) **31,** 4404–4414. doi:10.1038/emboj.2012.288; Published online 26 October 2012
Subject Categories: signal transduction; chromatin & transcription
Keywords: chromosome conformation capture; cytokine signalling; nuclear factor kappa B (NFκB); RNA polymerase; tumour necrosis factor alpha (TNFα); transcription factory

*Corresponding authors. Y Wada, Laboratory for Systems Biology and Medicine, Research Center for Advanced Science and Technology, University of Tokyo, 4-6-1 Komaba, Meguru-ku, Tokyo 153-8904, Japan. Tel.: +81 3 5452 5117; Fax: +81 3 5452 5117;
E-mail: wada-y@lsbm.org or PR Cook, Sir William Dunn School of Pathology, University of Oxford, South Parks Road, Oxford OX1 3RE, UK. Tel.: +44 (0)1865 275528; Fax: +44 (0)1865 275515;
E-mail: peter.cook@path.ox.ac.uk
[7]These authors contributed equally to this work.

Received: 26 April 2012; accepted: 24 September 2012; published online: 26 October 2012

Introduction

It is widely assumed that RNA polymerases transcribe by initiating on genes wherever they might be in a nucleus. However, accumulating evidence is consistent with an alternative: genes diffuse to dedicated sites—'transcription factories'—to be transcribed (Chakalova and Fraser, 2010; Cook, 2010). Transcription and associated RNA processing are enhanced by the high local concentration of relevant machinery in such a factory, which we define as a site containing at least two polymerases engaged on different templates. Strong support for this alternative is provided by chromosome conformation capture (3C) and fluorescence *in situ* hybridization (FISH): sequences distant on the genetic map often lie together in 3D nuclear space, and they are usually transcribed and/or associated with transcription factors (Osborne *et al*, 2004; Simonis *et al*, 2006; Fullwood *et al*, 2009; Göndör and Ohlsson, 2009; Yaffe and Tanay, 2011; Li *et al*, 2012). Moreover, each of the three nuclear RNA polymerases is concentrated in its own dedicated factories (Pombo *et al*, 1999), which can be purified as complexes of >8 MDa (Melnik *et al*, 2011). Polymerase II factories further specialize to transcribe different genes; two minichromosomes carrying identical units are transcribed in the same factories, but inserting into one a different promoter (or an intron) targets it to a different factory (Xu and Cook, 2008). In addition, factories transcribing genes encoding interleukins (Cai *et al*, 2006), cytochrome c subunits (Dhar *et al*, 2010), *Hox* genes (Noordermeer *et al*, 2011a), steroid receptor-binding genes (Fullwood *et al*, 2009; Grøntved and Hager, 2012), and factors involved in globin production (Brown *et al*, 2008; Schoenfelder *et al*, 2010; Soler *et al*, 2010; Noordermeer *et al*, 2011b) have been uncovered, as have associations of non-coding elements (Robyr *et al*, 2011). Here, we examine whether genes activated by a canonical signalling pathway congregate in factories specializing in transcribing responsive genes.

Tumour necrosis factor alpha (TNFα) is a potent cytokine that signals through nuclear factor kappa B (NFκB) to orchestrate the inflammatory response (Smale, 2010). NFκB is normally sequestered in the cytoplasm, but TNFα induces (via IKK-mediated phosphorylation and degradation of IκBs) phosphorylation of its p65 subunit, nuclear import, binding to cognate *cis* elements, and activation of responding genes (Ashall *et al*, 2009; Smale, 2010). Several hundred genes are activated within minutes, including *SAMD4A* and *EXT1* (Wada *et al*, 2009; Papantonis *et al*, 2010). If the traditional model for transcription applies, then there is no reason to expect responsive genes carried on different chromosomes to lie near these two genes in 3D space, either before or after TNFα induction. But if responsive genes are transcribed in specialized 'NFκB' factories, we would expect them to associate preferentially on stimulation (Figure 1). Using derivatives of 3C (de Wit and de Laat, 2012; Ethier *et al*, 2012)—a focussed one called variously 'circular 3C', '4C',

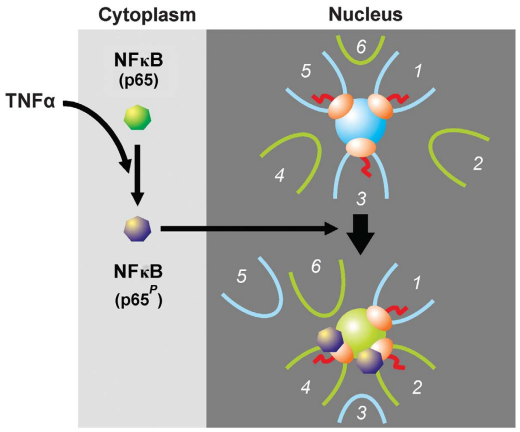

Figure 1 Hypothesis. NFκB (green) is usually cytoplasmic, and genes *1*, *3*, and *5* are transcribed in a factory (blue sphere) while TNFα-responsive genes *2*, *4* and *6* are unattached and inactive. Only 3 of the ~16 sequences attached to a factory are shown (Cook, 2010). TNFα induces phosphorylation of the p65 subunit of NFκB (now purple), import into the nucleus, binding to responsive promoters and/or the factory, and—once relevant promoters diffuse through the nucleoplasm and collide with the factory—transcription of responsive genes in what has become a 'specialized' factory (green sphere). As a result, gene *2* now lies near other responsive NFκB-binding genes. Gene *1* is still attached and transcribed, but may later be replaced by responsive gene *6*. If this model applies, then TNFα stimulation should bring gene *2* close to other responsive genes.

'3C-inverse PCR', or 'cACT' (Simonis *et al*, 2006; Zhao *et al*, 2006; Würtele and Chartrand, 2006; Papantonis *et al*, 2010) and one detecting a wider interactome called 'chromatin interaction analysis with paired-end tag sequencing' (ChIA-PET; Li *et al*, 2010)—we find most genes contacted by these two genes after stimulation to be TNFα responsive. Results are consistent with TNFα signalling through specialized 'NFκB' factories. As another cytokine—transforming growth factor β (TGFβ; Meulmeeste and Ten Dijke, 2011)—induces its responsive genes to associate, we suggest all cytokines will signal through specialized factories.

TNFα stimulation also downregulates many genes. As miRNAs are powerful downregulators, and as the nuclease (Drosha) involved in the initial step of miRNA processing acts co-transcriptionally (Morlando *et al*, 2008; Pawlicki and Steitz, 2008), we speculated that relevant pre-miRNAs are produced in 'miRNA' factories. We used the same strategy to see if genes hosting responsive miRNAs (Suárez *et al*, 2010) not only co-associated with other responsive genes, but also with genes hosting miRNAs; they did. This suggests that some 'NFκB' factories further specialize in producing non-coding transcripts regulating the inflammatory response.

Results

SAMD4A and EXT1 develop new contacts on stimulation

We apply 3C (Dekker *et al*, 2002) to detect proximity of two DNA sequences in 3D nuclear space, plus two variants producing more complete interactomes—a 4C variant using nested PCR (Papantonis *et al*, 2010) and ChIA-PET (Li *et al*, 2010). Our purpose is not to compile a complete interactome of responsive genes, but to focus on the principles governing co-association. Each approach has its own bias (introduced during amplification, cloning, immunoprecipitation, and/or DNA size selection prior to sequencing), but none should enrich for or against TNFα-responsive genes.

We first applied 4C to screen contacts made by two genes that respond promptly and synchronously to TNFα—*SAMD4A* (on HSA 14) and *EXT1* (on 8). Sixteen different 4C libraries were prepared at four different times after adding TNFα to HUVECs (i.e., 0, 10, 30, and 60 min), using *Sac*I or *Hin*dIII, and one of two reference points (the transcription start site, TSS, of *SAMD4A* or *EXT1*). Four more libraries were prepared after pretreatment with BAY 11-7085 (BAY), an indirect inhibitor of NFκB phosphorylation and so the signalling cascade (Pierce *et al*, 1997). 4C libraries were generated, cloned, and ~80 inserts per library sequenced (~48 for BAY libraries). This allowed analysis of inserts varying in length from 40 to >1000 bp, and—as conventional sequencing reads across ligation junctions—*bona fide* 3C products were verified. Less than 1% sequences in each library lacked appropriate restriction sites and were discarded. We also re-analysed *EXT1* and *SAMD4A* libraries (prepared with *Hin*dIII 0–60 and 30 min after stimulation, respectively) using 'next-generation' sequencing; amplified 4C products were re-cut, linkers attached, DNA fragments of 300 ± 100 bp selected, and ~10^7 (36-bp single-end) reads per library uniquely mapped to the genome.

The profile of *SAMD4A* and *EXT1* contacts changes on stimulation (Figure 2A). A minority of sequences in all libraries were 'unmapped' (mainly inserts <40 bp). At 0 min, most 4C products arise by self-ligation (ligation restores the original genomic sequence) or by ligation to nearby restriction sites within reference genes; we call all these 'intra-*SAMD4A*/-*EXT1*' contacts. Their presence is consistent with cut ends of each reference TSS lying far from other genes but close to other ends produced in these long genes of 221 and 312 kbp (as in Figure 1, *top*). This applies to most regions of the genome that make many local (*cis*) contacts on the same, but few (*trans*) contacts with other chromosomes (Lieberman-Aiden *et al*, 2009). But after 10 min, each (now-active) TSS often becomes ligated to DNA sequences lying within (or between) other RefSeq genes, many on different chromosomes (Supplementary Table S1). We call such contacts 'genic' (or 'non-genic'), and attribute the increase to the reference TSS binding to a factory surrounded by other genes (as in Figure 1, *bottom*). By 30 min, most contacts are genic ones (e.g., 21 and 26 different genic contacts were made by *SAMD4A* and *EXT1*, respectively, compared to 11 and 10 non-genic ones). BAY prevents development of these contacts (Figure 2A). We did not analyse non-genic contacts in detail, but they typically bind NFκB and possess histone marks indicative of active enhancers (Discussion).

On stimulation, contacts are with other TNFα-responsive genes

If factories specialize in transcribing responsive genes, then many new contacts should be with upregulated genes that bind both NFκB and active RNA polymerase II. To focus on frequent contacts, and mindful that 4C involves amplification that generates multiple identical clones of one 3C product, we require that all genic contacts analysed are seen on more than one occasion. Thus, after conventional sequencing, contacts must be seen in ⩾2 libraries or contact ⩾2 different parts of one gene; as expected, the two approaches detect partially

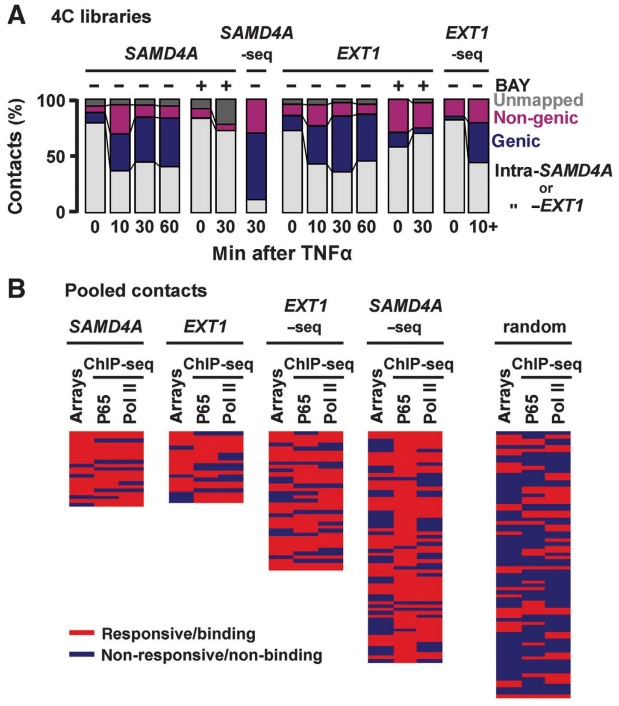

Figure 2 4C shows that TNFα induces *SAMD4A* and *EXT1* to associate with other responsive genes. HUVECs were grown in TNFα for 0–60 min (± BAY 11-7085, 'BAY'—an inhibitor of p65 phosphorylation), and 4C applied. (**A**) Evolving contacts in 20 4C libraries. Reference gene, BAY pretreatment, and time after stimulation are indicated. Results from libraries prepared using *Sac*I or *Hin*dIII are pooled. Some *Hin*dIII libraries were also analysed by high-throughput sequencing ('*EXT1*-/*SAMD4A*-seq', with results of 10–60 min *EXT1* libraries pooled and labelled as '10+'). At 0 min, most contacts are 'intra-*SAMD4A*/-*EXT1*'. After 10 min, contacts develop with non-genic and genic regions; by 30 and 60 min, most are with other genic regions. Pretreatment with BAY prevents this evolution. (**B**) Most contacts (detected on ⩾2 independent occasions between 10 and 60 min) are with responding, p65-binding, genes. Genes were scored as TNFα responsive (⩾1.5-fold change compared to 0-min levels, determined using publicly available microarray data) and able to bind the p65 subunit of NFκB or RNA polymerase II (red), or non-responsive/non-binding (blue; determined using ChIP-seq here). Each row gives results for one gene; a set of 75 randomly selected human genes is presented for comparison (genes listed in rank order of decreasing number of contacts, as in Supplementary Tables S1 and S2). In all, 57% contacts ($n=21$) made by *SAMD4A* (39% by *EXT1*-seq; $n=57$) are with genes that are responsive and bind both p65 and the polymerase; the value for the random set (7%; $n=75$) is significantly lower ($P<0.0001$ in both cases; two-tailed Fisher's exact test).

overlapping contacts (Supplementary Tables S1 and S2). We determined whether each contacted gene was TNFα responsive using microarray data (Materials and methods), and chromatin immunoprecipitation coupled to next-generation sequencing (ChIP-seq), was used to assess whether contacted genes also bind the p65 subunit of NFκB and phosphorylated isoforms of polymerase II; a randomly generated set of 75 human genes (which represent the complete range of activity) serves as a control (Figure 2B; Supplementary Tables S1 and S2). As significantly more contacts made by *SAMD4A* and *EXT1* are with genes that are both responsive and/or have p65 and/or the polymerase bound to their promoters, the two reference genes mostly contact other responsive/p65-binding genes.

Responsiveness assessed using microarray data reflects changes in steady-state mRNA levels occurring over hours; however, changes in nascent RNAs occurring within minutes are of interest here. Therefore, we monitored such changes using intronic qRT–PCR; we also assessed p65 and RNA polymerase binding by ChIP. Three sets of 12 genic contacts seen after stimulation were randomly selected for detailed analysis; a random set provides a control (Supplementary Table S1). Almost all genes in the experimental sets were upregulated and had p65 and the polymerase bound to their promoters, and BAY abolished this (Supplementary Figures S1A, B and S2A, C, D). Note also that binding of p65 to ~1/3 of these genes depends on ongoing transcription (it is inhibited by elongation-inhibitor DRB; Supplementary Figure S2B), and that most of the genes are expressed at levels comparable to *GAPDH* (Supplementary Figure S3A). Moreover, 4C contacts strongly correlate with the number of p65 binding sites on different chromosomes ($R=0.75$; Supplementary Figure S3B). Taken together, results are consistent with responsive genes associating on activation, and with their contacts evolving thereafter (for an overview, see Supplementary Figure S4).

TNFα-responsive genes encoding miRNAs co-associate

The above analysis concentrates on coding genes; what of non-coding ones? Speculating that TNFα-responsive pre-miRNAs are produced in discrete 'miRNA' factories, we applied the same strategy to see if three genes hosting responsive miRNAs (encoding miR-17, -155, and -191; Suárez *et al*, 2010) not only came together with other responsive genes, but also with ones hosting miRNAs. As only ~1500 of the ~22 000 human genes are currently known to host miRNAs (Dweep *et al*, 2011), random co-association of miRNA genes is unlikely. First, qRT–PCR confirmed that TNFα induces transcription of miR-17, -155, and -191 precursors in HUVECs, but not of non-responsive miR-15α (Figure 3A). 3C then revealed that *MIR17HG* (on HSA 13) contacts none of the others before adding TNFα. However, 30 min after stimulation it contacts *MIR155HG* (on 21) and *MIR191* (it lies within *DALRD3* on 3), but not non-responsive *MIR15A* (on 13; Figure 3B).

We next used 4C to screen for other contacting sequences. Three new libraries were generated 30 min after stimulation using *MIR17HG*, *MIR155HG*, or *MIR191* as reference points, and 96 inserts in each sequenced. Most contacts (seen at least twice) made by each of the three references were with genic sequences that were TNFα responsive and/or able to bind p65 and/or the polymerase (Figure 3C); this confirms the principle that responding genes co-associate on stimulation. Moreover, ~1/3 contacts encoded miRNAs (Figure 3C, *arrowheads*), and 70% of these were upregulated by TNFα in a BAY-sensitive manner (Supplementary Figure S1C). Results indicate that a subset of responding genes encoding miRNAs also co-associate on activation (for an overview, see Supplementary Figure S4 and Supplementary Table S3).

Finally, if TNFα signalling led to mRNA downregulation by activating production of miRNAs encoded by our three references and their contacts, downregulated mRNAs should be enriched with binding sites for these miRNAs (Guo *et al*, 2010). They appear to be, as the 100 mRNAs most downregulated 1 and 4 h after stimulation contain more potential binding sites than a random set (Supplementary Table S4). This supports the idea that miRNAs encoded by co-associating genes are functionally relevant.

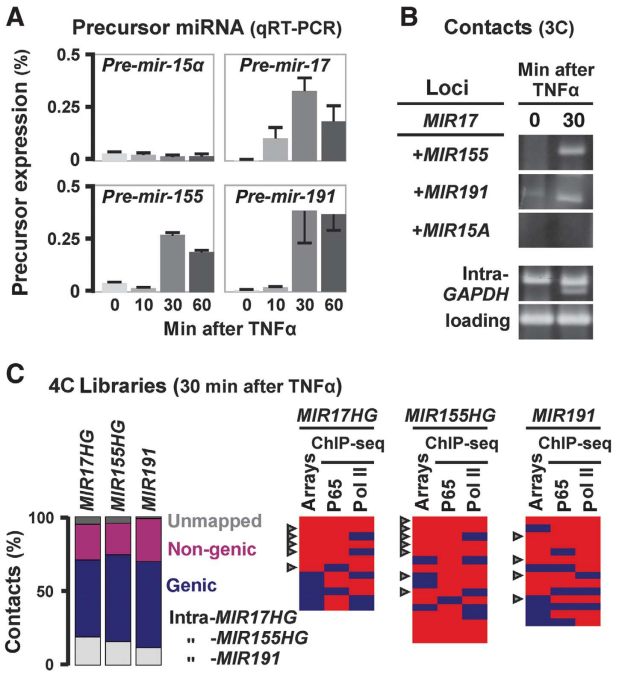

Figure 3 TNFα-responsive genes hosting miRNAs co-associate. HUVECs were grown in TNFα (0–60 min), total nucleic acids purified and 3C/4C applied. (**A**) Levels of precursor miRNAs assessed by qRT–PCR (normalized relative to *RNU6* RNA; ± s.d.; $n=3$). Levels of (non-responsive) miR-15α remain unchanged; those of the three other miRNAs peak after 30 min. (**B**) Responsive miRNA host genes co-associate. 3C reveals that *MIR17* (on HSA 13) contacts *MIR155* (on 21) and *MIR191* (on 3) after 30 min (but not at 0 min); it does not contact *MIR15A* (on 13) at either time. Bands reflect contacts, and controls for intra-*GAPDH* contacts and loading are shown. (**C**) *MIR17HG*, *MIR155HG*, and *MIR191* often contact other responsive genes that bind p65. 4C libraries were generated 30 min after stimulation and ~96 inserts in each sequenced. *Left:* Bar graphs illustrate types of contact seen. *Right:* Genic contacts seen at least twice are listed in rank order of those seen most frequently (see also Supplementary Table S3). These were then scored (as in Figure 2B) as responsive and/or able to bind the p65 subunit of NFκB and/or RNA polymerase II (red), or unresponsive/non-binding (blue). *Arrowhead*: miRNA host gene. The observed high frequency of contacts with genes hosting miRNAs (43%; $n=42$) is significant, as only 6 such contacts are seen in the 228 contacts of the *SAMD4A* and *EXT1* protein-coding genes (Supplementary Tables S1 and S2), and as only 1424 such genes are known (out of ~22 000 RefSeq genes; $P<0.0001$ in both cases; two-tailed Fisher's exact test). In all, 33% contacts made by *MIR17HG* ($n=12$), 50% by *MIR155HG* ($n=16$), and 36% by *MIR191* ($n=14$) are with genes that are TNFα responsive and bind both p65 and the polymerase—significantly more than the 7% ($n=75$) seen with the random set in Figure 2B ($P=0.019$, 0.0001, and 0.0076, respectively; two-tailed Fisher's exact test). Figure source data can be found with the Supplementary data.

Nascent RNAs and pre-miRNAs encoded by responsive genes colocalize

We used RNA FISH with intronic probes to confirm that nascent RNAs encoded by frequently contacting genes lie together. As stochasticity in transcription ensures both alleles of most human genes are rarely transcribed simultaneously (Chubb and Liverpool, 2010)—including *SAMD4A* and *EXT1* (Wada *et al*, 2009; Papantonis *et al*, 2010)—we used a multiplexed set of probes targeting intronic RNA encoded by seven different genes (three *cis* and four *trans*, to *SAMD4A*; Materials and methods) paired with: (i) a probe targeting *SAMD4A* intron 1 or (ii) a (control) probe targeting *EDN1* intron 2 (a constitutive, non-responsive, gene with comparable activity to *SAMD4A*; Wada *et al*, 2009). Note that (diploid) HUVECs are starved prior to stimulation so essentially all cells are in the G0 phase of the cell cycle (Larkin *et al*, 2012), and ~35% *SAMD4A* alleles plus ~10–30% alleles of each of the seven contacted genes in a population are active after stimulation. RNA FISH yields three types of foci: red ones mark nascent transcripts copied from alleles of one or more of the seven multiplexed targets, green ones mark *SAMD4A* nascent RNA, and yellow ones indicate colocalization of two (rarely two pairs of two) nascent transcripts (see Materials and methods for colocalization criteria). In all, 60% green foci colocalized with at least one red focus to give such yellow foci, significantly higher than the ~2% colocalization seen with *EDN1* (Figure 4A, i and ii). Similar results are seen with the same probes 60 min after stimulation (Figure 4A, iii–vi), with a responsive gene with a different interactome—*EXT1* (Supplementary Tables S1 and S2), and another constitutively expressed control gene—*RCOR1*—on the same chromosome as *SAMD4A* (with activity comparable to *GAPDH*; Papantonis *et al*, 2010). Analogous results were obtained when *SAMD4A* was paired with four multiplexed probes targeting genes on four other chromosomes (29% colocalization), and by DNA FISH on two responsive loci (5% colocalization; Supplementary Figure S5A). Similarly, nascent RNA encoded by responsive *MIR155HG* colocalizes with nascent RNAs from eight *MIR155HG* contacts (Figure 4A, vii and viii). These confirm 4C results; if genes co-associate, so do their nascent transcripts. As many red and green foci do not colocalize (e.g., of 181 *SAMD4A* green foci analysed 30 min post induction, 27% did not overlap any red focus, 57% overlapped a single red focus, and only 16% colocalized with ⩾2 red foci), it also follows there must be many factories specializing in transcribing responsive genes in one cell (see Discussion).

Nascent SAMD4A and EXT1 transcripts are found in 'NFκB' factories

Electron and high-resolution light microscopy reveal that nascent transcripts lie on the surface of ~90 nm factories (Eskiw *et al*, 2008; Papantonis *et al*, 2010; Larkin *et al*, 2012). We measured separations between colocalizing red and green signals (like those in Figure 4A) given by *SAMD4A* and the multiplexed genes using high-resolution microscopy (with 22-nm precision, and so well below the resolution limit). We assume a yellow focus marks subdiffraction red/green spots, fit Gaussian profiles to intensities, and measure the separation between peaks. A 'perfectly' colocalizing control—red/green fluorescent beads—yields separations of <25 nm (Figure 4B, *inset*), as expected of randomly oriented fluors in a small sphere localized with the measured precision. Experimentally measured separations were broadly distributed up to 160 nm (Figure 4B). This distribution is the one expected of a model (Papantonis *et al*, 2010) where pairs of red and green spots are randomly and repeatedly distributed in a 35-nm shell around a 90-nm core—the known dimensions of a factory (Figure 4B, compare orange and blue curves).

As TNFα induces phosphorylation of the p65 subunit of NFκB and nuclear import (Ashall *et al*, 2009), we might expect to find $p65^{P}$ in factories transcribing responsive genes (Figure 1). Four results support this: $p65^{P}$ appears within 10 min in discrete nuclear foci in a BAY-sensitive manner (Supplementary Figure S5B), it co-purifies with

large fragments of factories released from nuclei by caspases (Melnik *et al*, 2011; Supplementary Figure S5C), and it is associated with both nascent RNAs encoded by *SAMD4A* and *EXT1* (Supplementary Figure S5D) and foci containing nascent BrRNA (Supplementary Figure S5E). Thus, nascent RNAs are produced in transcriptionally active sites rich in 'active' NFκB.

ChIA-PET confirms co-association of responsive genes

4C reveals interactomes of selected genes; ChIA-PET permits a wider analysis. We prepared two more libraries (0 and 30 min after adding TNFα) by immunoselecting chromatin bound to phosphorylated isoforms of RNA polymerase II, and generated genome-wide interactomes using next-generation sequencing ($\sim 3.5 \times 10^7$ paired-end reads per library, from which $\sim 10^7$ were uniquely mapped to the genome). To minimize amplification effects, two or more reads that were identical (or mapped ±2 bp of one another) were classified as one PET; thus, most PETs/contacts are represented by numerous reads. We analysed frequent contacts made by *SAMD4A*, *EXT1*, plus the three miRNA reference genes. (Results for the miRNA genes were pooled as each made few contacts—which we attribute to poor immunoselection due to low transcription rates (which are 1:0.45:0.2 for *SAMD4A*, *EXT1*, and *MIR155HG* as assessed by nascent RNA FISH)). On stimulation, the fraction of genic contacts increases, with the number of contacts seen being in the order *SAMD4A* > *EXT1* > miRNAs (again reflecting transcription rates; Supplementary Figure S6A). Most contacts after stimulation are again with responsive genes that bind p65 and/or the polymerase (Figure 5A), and a number of these encode miRNAs and/or ncRNAs (Figure 5A, *arrowheads*). These results confirm that stimulation induces responding genes to co-associate (for an overview, see Supplementary Figure S6B and Supplementary Tables S5 and S6).

To extend analysis to more genes, we selected the 69 most upregulated by TNFα after 60 min (using microarray data), and determined whether stimulation increased contacts between them; it did (Figure 5B). These contacts do not simply result from transfer of active genes to an open (active) chromatin compartment, as the 69 made significantly fewer contacts with the 69 most highly active, but non-responsive, genes (Figure 5B), or with sets of 69 constitutive or TGFβ-responsive genes (Supplementary Figure S6C). Importantly, the number of interactions between the 69 genes most upregulated by TNFα was significantly higher than that seen between the 69 highly active, non-responsive, genes (Supplementary Figure S6C), suggesting some sort of specialized spatial coordination of associations.

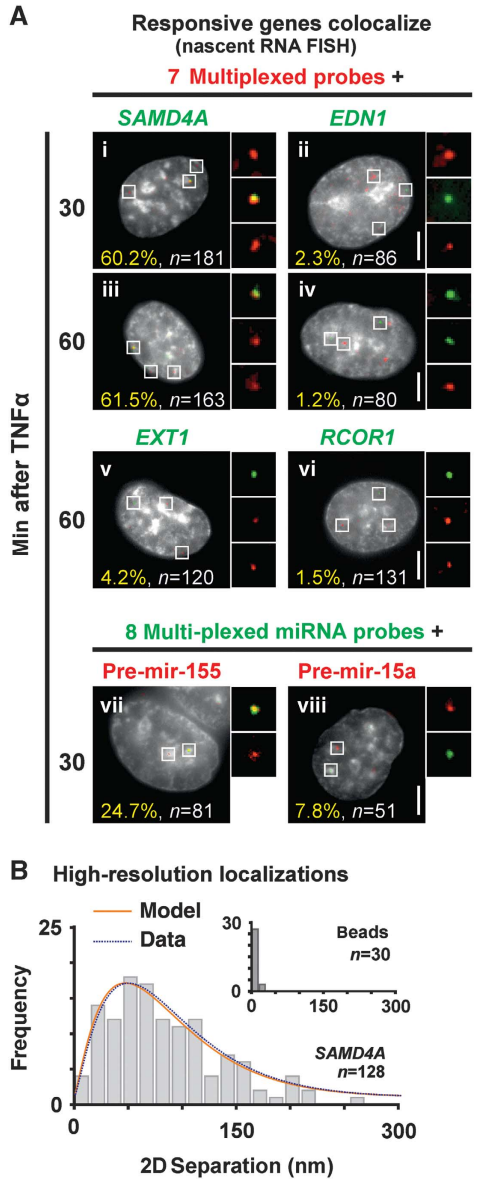

Figure 4 RNA FISH shows colocalization of nascent RNAs encoded by responsive genes in structures the size of factories. HUVECs were stimulated with TNFα, fixed, nascent transcripts detected using RNA FISH, DAPI-stained cells imaged, and distances between overlapping red and green signals measured using high-resolution localization. (**A**) Typical images (insets show magnifications of selected foci). *Bars*: 2 μm. (i–iv) A green probe targets nascent RNA encoded by *SAMD4A* (or *EDN1*, a non-contacted, non-responsive, control on HSA 6 with a comparable activity to *SAMD4A*), while a multiplexed set of red probes targets intronic RNA encoded by seven different genes (targeting regions >0.5 Mbp away from *SAMD4A*, or on different chromosomes). Approximately 60% *SAMD4A* foci (green) colocalize with a red focus (which might contain 1–7 targets) to give a yellow one; significantly fewer *EDN1* foci (green) colocalize with red foci ($P<0.0001$; two-tailed Fisher's exact test). (v, vi) Similar results were obtained when *EXT1* (a responsive gene on HSA 8 that has a different interactome from *SAMD4A*; see Supplementary Tables S1 and S2) or *RCOR1* (a non-contacted, non-responsive control on the same chromosome as *SAMD4A* that has an activity comparable to *GAPDH*) was used together with the seven multiplexed *SAMD4A*-contacting targets ($P<0.0001$ in both cases; two-tailed Fisher's exact test). (vii, viii) A red probe targets nascent pre-miR-155 or pre-miR-15a RNA (a non-responsive control), while a multiplexed set of green probes targets eight different nascent pre-miRNAs (all 4C contacts of *MIR155HG*). Approximately 25% pre-miR-155 foci (red) colocalize with green foci; significantly fewer pre-miR-15a (red) foci colocalize with green foci ($P=0.019$; two-tailed Fisher's exact test). (**B**) High-resolution localization (22-nm precision). Yellow foci like those in (**A**) were selected (*n* gives number of foci analysed), and separations between peaks in red and green channels measured. The histogram gives frequencies of separations, the blue curve is a gamma-fit to this histogram, and the orange one the distribution expected if pairs of red and green points are randomly distributed in a 35-nm shell around a 90-nm sphere (Papantonis *et al*, 2010). *Inset*: separations between peaks given by red/green fluorescent 110-nm beads used as colocalizing controls.

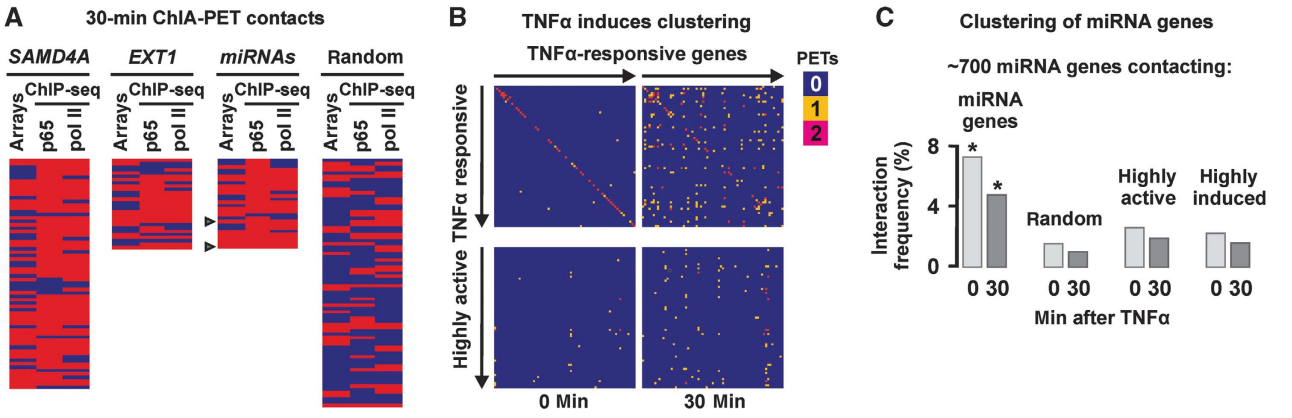

Figure 5 ChIA-PET confirms that TNFα-responsive genes, and those encoding miRNAs, co-associate. HUVECs were grown in TNFα for 0 or 30 min, active RNA polymerase II immuno-selected, ChIA-PET performed, and the interactions between selected genes were analysed. The statistical significance of differences was assessed using two-tailed Fisher's exact test in (**A**, **B**) or χ^2 test with Yates' correction in (**C**). (**A**) Most genic contacts made by *SAMD4A*, *EXT1*, and three miRNA genes at 30 min are TNFα responsive and p65 binding. Contacted genes (with $\geqslant 3$ or $\geqslant 2$ PETs/contacts each, for *SAMD4A*/*EXT1* and miRNA genes, respectively) are shown in rank order (of those more frequently seen) and scored as responsive/binding (red) or non-responsive/non-binding (blue) as in Figure 2B. Arrowhead: gene hosting two miRNAs. In all, 49% contacts made by *SAMD4A* ($n=68$), 36% by *EXT1* ($n=28$), and 46% by miRNA genes ($n=28$) are TNFα responsive and bind both p65 and the polymerase—a significant enrichment ($P<0.0001$, 0.0006, and <0.0001, respectively) compared to the random set (7%; $n=75$). The observed frequency of contacts hosting miRNAs (14%; $n=28$) is significantly higher than for *SAMD4A* and *EXT1* (3%; $n=228$; $P=0.015$). (**B**) Contacts made by the 69 genes most upregulated by TNFα. Coloured boxes indicate 0 (blue), 1 (yellow), or $\geqslant 2$ (red) contacts/PETs between two genes. *Top*: Genes are ranked in order of upregulation by TNFα (left to right and top to bottom; all $\geqslant 1.9$-fold, determined using microarrays 0 and 60 min after stimulation). Significantly, more contacts develop after 30 min ($P<0.0001$). *Bottom*: The same 69 most upregulated genes versus the 69 most highly expressed, but non-responsive genes (all ± 1.5-fold, determined as above); after 30 min, there are significantly fewer contacts ($P<0.0001$) than in the 30-min matrix above (additional controls in Supplementary Figure S6). (**C**) Genes encoding miRNAs tend to contact each other before and after stimulation (assessed using PETs/contacts made by >700 genes encoding miRNAs). The interaction frequency (%) is the number of PETs divided by the number of possible pairwise combinations. *Significantly more contacts are seen between the ~700 miRNA genes (*left*; $P<0.0001$), compared to the ~700 miRNA genes with the same number of randomly selected, highly expressed, or induced genes.

Unfortunately, there remains no genome-wide data on miRNAs upregulated by TNFα, so we could only use the ChIA-PET data to examine whether genes hosting miRNAs co-associate before and after stimulation (and not how stimulation influences co-association). We compiled a list of 20 upregulated miRNA-encoding genes from microarray (Suárez *et al*, 2010) and qRT–PCR data (Supplementary Figure S1C) and examined their interactomes. They yielded many more contacts amongst themselves, compared to those they made with 20 constitutively expressed miRNA genes, or with 20 miRNA-hosting genes upregulated by another cytokine—vascular endothelial growth factor (VEGF; Supplementary Figure S6E; Suárez *et al*, 2008). Finally, we examined all ~700 miRNA-hosting genes that yielded $\geqslant 1$ PET/contact. We compared contacts they made at 0 or 30 min either with each other, or with a set of randomly selected genes. At both times, the interaction frequency between the ~700 was higher than between the ~700 and control groups of highly active or highly induced coding genes (Figure 5C). These results confirm that genes hosting miRNAs tend to congregate (see additional controls in Supplementary Figure S6F).

Does TGFβ signal through specialized factories?

Finally, we examined whether a different cytokine—TGFβ$_1$—uses the same strategy as TNFα. TGFβ plays a critical role in tumour development (Meulmeeste and Ten Dijke, 2011) and signals through the SMAD family of transcription factors to activate transcription of many genes, including *ETS2* on HSA 21 (Koinuma *et al*, 2009a, b). Two new 4C libraries were prepared from HUVECs harvested 0 and 60 min after TGFβ$_1$ stimulation, using the TSS of *ETS2* as a reference point. Once again, genic contacts develop (Figure 6A and B), many contacts bound SMADs (Figure 6A; binding assessed using published data; Koinuma *et al*, 2009a, b), and most contacts seen at least twice were TGFβ responsive (Figure 6C). Moreover, one-third of these contacted genes also respond to TNFα, consistent with some overlap between the two pathways (Sullivan *et al*, 2009; Supplementary Table S7). In contrast, a random (control) set contains significantly fewer genes able to respond to either cytokine or bind SMADs (Figure 6A). These results support the idea that TGFβ signals through specialized 'SMAD' factories.

Discussion

TNFα orchestrates the inflammatory response by signalling through NFκB to activate and repress many genes (Smale, 2010). Two protein-coding (*SAMD4A* and *EXT1*) and three miRNA-hosting genes (*MIR17HG*, *MIR155HG*, and *MIR191*) are among the first to respond; we use these as reference points and examine whether TNFα-responsive genes are co-transcribed in 'NFκB' factories (Figure 1). Before stimulation, 4C and ChIA-PET reveal reference genes contact few others, but after 10–60 min they mainly contact genes that are responsive and/or bind NFκB and/or active isoforms of the polymerase (Figures 2, 3, and 5). Contacts do not simply result from transfer of active genes to an active chromatin compartment, as there were significantly fewer contacts with other highly active, non-responsive, genes (Figure 5B; Supplementary Figure S6C). RNA FISH (applied with intronic probes and coupled to high-resolution microscopy) confirms that nascent transcripts encoded by these responsive genes

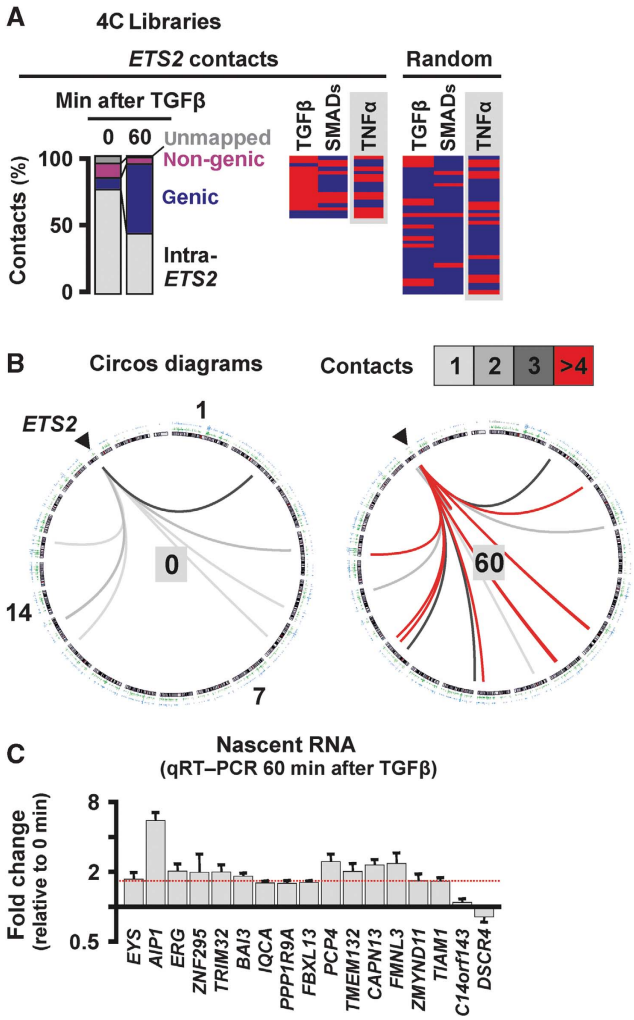

Figure 6 TGFβ induces responsive *ETS2* to associate with other TGFβ-responsive genes. 4C libraries were prepared from HUVECs harvested 0 or 60 min after stimulation with TGFβ, using *Hin*dIII and the TSS of *ETS2* as a reference point; 95 and 196 inserts from the 0- and 60-min libraries were sequenced, respectively. Total RNA was also isolated, and levels of nascent RNA encoded by some contacts assessed (using qRT–PCR with intronic probes). (**A**) 4C libraries. *Left*: Contacts classified as in Figure 2A; initially most are 'intra-*ETS2*', but then more genic contacts develop. *Right*: Genic contacts seen at least twice (listed in rank order of number of contacts) were scored as responsive/binding (red), or unresponsive/non-binding (blue) as in Figure 2B. In all, 35% contacts ($n=17$) both respond to TGFβ and associate with SMADs (assessed using published ChIP data; Koinuma *et al*, 2009a, b), significantly more than the 3% ($n=36$; Supplementary Table S7) in the control set ($P=0.003$; two-tailed Fisher's exact test), consistent with TGFβ-responsive genes being co-transcribed in specialized 'SMAD' factories. *Grey rectangles*: some TGFβ-responsive contacts also respond to TNFα. (**B**) Circos software was used to depict *ETS2* (on HSA 21, *arrowhead*) contacts evolving over time. *Inner circle*: chromosome ideograms drawn clockwise from 1 to Y. *Outer circles*: two sets of SMAD ChIP data (Koinuma *et al*, 2009a, b). *Interior*: contacts made by *ETS2* (box indicates numbers) increase after 60 min, and are mainly with sites binding SMADs. (**C**) Responsiveness of all genes contacted by *ETS2* after stimulation (and seen at least twice) assessed using qRT–PCR. The fold change in nascent RNA expression levels (relative to 0 min) is presented. In all, 71% contacted genes are upregulated ⩾1.5-fold (indicated by red dotted line).

often lie together on the surface of 90-nm factories (Figure 4). Could these genes/transcripts associate with some structure other than a factory—for example, a nuclear 'speckle' that is known to lie near nascent RNA (Brown *et al*, 2008; Spector and Lamond, 2011)? It seems unlikely, as speckles are themselves transcriptionally inactive (Pombo and Cook, 1996) and have larger diameters (i.e., 0.5–3 μm; Hall *et al*, 2006) inconsistent with the profile seen in Figure 4B. While incompletely spliced transcripts can associate with speckles (Hall *et al*, 2006; Spector and Lamond, 2011), *SAMD4A* transcripts are spliced co-transcriptionally (Wada *et al*, 2009) so FISH signals in Figure 4A should mark transcription sites.

Some factories further specialize in producing miRNAs that target downregulated mRNAs (Figure 3; Supplementary Table S4). And even before stimulation, about half the genes encoding miRNAs tend to be co-transcribed in factories specializing in miRNA production (Figure 5C) which—presumably—contains high concentrations of Drosha, the nuclease that co-transcriptionally cleaves the miRNA precursor (Morlando *et al*, 2008).

These results beg many questions, such as: (i) are responsive genes poised prior to activation at/near factories (Nechaev and Adelman, 2008; Ferrai *et al*, 2010) so as to respond rapidly? Although *SAMD4A* and *EXT1* make few genic contacts before stimulation, almost half are also detected after stimulation (Supplementary Table S1). Most are preloaded with RNA polymerase II (Supplementary Figure S2D) and have the potential to respond to TNFα and bind p65 (Supplementary Figures S1A, B and S2A, C). Before stimulation, we imagine that potentially responding genes lie near preexisting 'naive' factories, which they visit every few minutes as they diffuse through the nucleoplasm. Occasionally, promoters might transiently bind to polymerases in a factory, but few initiate as the concentration of relevant transcription factors is low. When stimulation induces nuclear influx of phospho-NFκB (Supplementary Figure S5B), the factor binds to responsive promoters and stabilizes attachment to a factory. Once productive transcription begins, responsive genes become tethered to the factory, and so our reference genes have a high probability of contacting them. As more responsive genes bind and the local NFκB concentration increases, the factory evolves into one that predominantly—but not exclusively—transcribes TNFα-responding genes. We currently favour this model over one involving *de novo* formation of specialized factories as some responding genes are associated with existing factories before stimulation (see also Mitchell and Fraser, 2008), and as transcription seems to be required for p65 binding to some responsive promoters (Supplementary Figure S2B). (ii) Do non-genic contacts differ from genic ones? Due to better annotation we concentrated on genic contacts, but preliminary analysis indicates that non-genic contacts are transcriptionally active and bind p65, and so might be enhancers. In all, 8 of the 10 non-genic contacts seen most frequently in all 20 (4C) *SAMD4A/EXT1* libraries both possess histone marks characteristic of active enhancers (i.e., H3K27ac and H3K4me1; Zentner *et al*, 2011) and p65 binding increases on stimulation (Supplementary Figure S3C). We suggest such contacts reflect promoter–enhancer interactions (Lomvardas *et al*, 2006; Apostolou and Thanos, 2008) tethering TNFα-responsive promoters close to relevant 'NFκB' factories (Kolovos *et al*, 2012). Note also that ~9% non-genic contacts made by the three reference genes hosting miRNAs encode non-coding RNAs (Supplementary Tables S3 and S6). (iii) How many 'NFκB' factories might *SAMD4A* access, and

what is the total number of 'NFκB' factories per nucleus? We can only speculate, but estimate *SAMD4A* can access ~8 of the 150–250 'NFκB' factories—a subset of the ~2200 polymerase II factories (for details, see Supplementary Methods and Supplementary Figure S6D). (iv) How many different types of specialized factories might there be? Again, we can only speculate, but suggest a factory specializing in transcribing genes responding to one cytokine may also transcribe some genes responding to a related cytokine, as TNFα- and TGFβ-responding reference genes contact some responding to both (Figure 6; Supplementary Table S7). Such overlapping specialization clearly allows outputs of inter-linked pathways to be integrated through transcription of genes encoding co-regulators. And as the clusters of genes associated with factories evolve after stimulation (Supplementary Figures S4 and S6B) there are rich possibilities for multi-tiered temporal regulation.

Materials and methods

Cell culture

HUVECs from pooled donors (Lonza) were grown to ~90% confluence in Endothelial Basal Medium 2-MV with supplements (EBM; Lonza), starved (16 h) in EBM + 0.5% FBS, and treated with TNFα or $TGF\beta_1$ (10 or 50 ng/ml, respectively; Peprotech) for 0–60 min. In some cases, 10 μM BAY 11-7085 (Sigma-Aldrich) or 50 μM 5,6-dichloro-1-β-D-ribo-furanosyl-benzimidazole (DRB; Sigma-Aldrich) was added 1 h before and retained after stimulation.

Chromosome conformation capture (3C)

3C was performed as described, until DNA purification (step 23; Göndör *et al*, 2008). In brief, 10^7 cells were fixed (1% paraformaldehyde; 10 min; 20°C; Electron Microscopy Sciences), aliquots of 10^6 cells in 0.125 M glycine/PBS spun, cells resuspended in the appropriate restriction enzyme buffer and lysed (16 h; 37°C) in 0.3% SDS. After sequestering SDS using 1.8% Triton X-100 (1.5 h; 37°C), cells were treated overnight with *Hin*dIII or *Sac*I (800 units added in 4 sequential steps; New England Biolabs), the enzyme heat inactivated (25 min; 65°C), and digestion efficiency determined by quantitative PCR (qPCR); samples with digestion efficiencies >75% were ligated using T4 ligase (6000 units; New England Biolabs; DNA concentration <0.6 ng/μl; 72 h, 4°C to minimize unwanted ligations) and crosslinks reversed (16 h; 65°C) in proteinase K (10 mg/ml; New England Biolabs) before DNA was purified using an EZNA MicroElute DNA clean-up kit (Omega BioTek) and a PCR Purification kit (Qiagen). Non-digested/ligated and digested/non-ligated templates were also prepared. For 3C-PCRs, amplification efficiency controls using bacterial artificial chromosomes were as before (Papantonis *et al*, 2010). Identity of 3C bands was verified by sequencing (SourceBioscience, Oxford).

4C and 4C-seq

4C was based on 3C-inverse PCR/circular 3C (Simonis *et al*, 2006; Zhao *et al*, 2006; Würtele and Chartrand, 2006). Approximately, 1 μg 3C template (i.e., isolated DNA with crosslinks reversed, prepared as above) was cut with *Csp*6I (80 units; Invitrogen), diluted and self-ligated in 1 ml (16 h; 4°C) using T4 DNA ligase (400 units), and purified (EZNA MicroElute DNA clean-up kit); 1/50th eluate was then used in nested inverse PCR (for external primers: 95°C/2 min, plus 13 cycles at 95°C/50 s, 56°C/45 s, and 72°C/2 min, followed by a cycle at 72°C/5 min; for internal primers: 95°C/2 min, 18 cycles at 95°C/50 s, 60°C/35 s, and 72°C/1.5 min, followed by a cycle at 72°C/4 min) using GoTaq polymerase (Promega) in 2.5% dimethylsulphoxide. For conventional sequencing, amplimers were resolved on 1.5% agarose gels stained with SYBR Green stain I (Invitrogen), gel slices spanning sizes 0–100, 100–250, 250–500, 500–750, and >750 bp excised, DNA purified from each (EZNA MicroElute kit) and cloned into pGEM-T (Promega). TOP10 cells (Invitrogen) were then transformed with a 1:1:1:1:1 (1 μl each) mixture of ligation reactions, and plasmid inserts sequenced (SourceBioscience, Oxford). Inserts flanked by *SAMD4A*/*EXT1* sequences and *Hin*dIII/*Sac*I-*Csp*6I restriction sites were mapped to the human genome (hg18) using BLAST (mask: low complexity; expect value: 0.1). In all, 755 clones were sequenced for *SAMD4A* (144, 182, 172, 161, 48, and 48 for 0, 10, 30, 60 min, 0 min + BAY, and 30 min + BAY libraries, respectively), 745 clones for *EXT1* (183, 140, 181, 139, 52, and 50 for 0, 10, 30, 60 min, 0 min + BAY, and 30 min + BAY libraries, respectively), and 374 clones for *ETS2* (148 and 226, for 0 and 60 min, respectively). Numbers of clones analysed at a particular time are pooled from two independent experiments; Supplementary Figure S7 illustrates reproducibility obtained with different experiments/libraries. In all, <1% sequences in each library were not flanked by appropriate sequence motifs and were not analysed. 4C showed high reproducibility when ~80 inserts or more were read by conventional sequencing, e.g., in the *ETS2* libraries prepared 60 min after stimulation using *Hin*dIII ~75% sequences were shared between two replicates (not including self-ligated inserts; Supplementary Figure S7A). Reproducibility was adequate even when different enzymes were used to generate libraries (e.g., ~39% sequences were shared between *SAMD4A* libraries prepared using *Sac*I and *Hin*dIII, 10 min after stimulation; Supplementary Figure S7A). For next-generation sequencing, >10 ng DNA was processed as per manufacturer's instructions (Illumina). Briefly, amplimers were re-cut with *Hin*dIII and *Csp*6I, electrophoretic profiles evaluated using Bioanalyzer (Agilent Technologies), ends repaired and linkers ligated, products separated on agarose gels and fragments of 300 ± 100 bp re-purified. From each library, $\sim 15 \times 10^6$ 36-bp single-end reads were obtained, ~70% of which contained one or other restriction site. After eliminating the first 5 bases containing the restriction-enzyme motif, ~97% resulting 31-base reads were successfully aligned to 175 (0 min), 269 (10 min), 723 (30 min), and 258 (60 min) unique loci in the human genome (hg18) allowing <2 mismatches (multiple mappings and mappings to repeat elements disallowed). Reads within 5 kbp (the average *Hin*dIII restriction fragment size) of a RefSeq gene were categorized as genic, and ranked according to the number of unique mapping sites (all such genic contacts are listed in Supplementary Table S2; typical genome browser view in Supplementary Figure S8A). To focus on frequent contacts, we selected only those represented by ⩾2 sites of ⩾10 identical reads mapping to one RefSeq gene. The number of reads mapping to one site varied greatly (i.e., from 1 to 2.5×10^6). When contacts were compared to those seen by conventional sequencing an overlap of ~25% was observed (Supplementary Figure S7B). 4C-seq data are available in the Sequence Read Archive (NCBI) under accession numbers SRX045413.2, SRX045414.2, SRX045412.3, and SRX045415.3.

Chromatin interaction analysis with paired-end tag sequencing

ChIA-PET was as described (Li *et al*, 2010). Briefly, confluent HUVECs were serum-starved (16 h), treated (0–30 min) with TNFα, crosslinked using 10 mM ethyl-glycol-*bis*-succinimidylsuccinate (EGS; Thermo Scientific) in 50% glacial acetic acid (45 min) and then in 1% paraformaldehyde (20 min; TAAB), quenched (5 min) in 2.5 M glycine, harvested, sonicated (Branson), and ChIP performed using magnetic beads (Invitrogen) and the Pd75C9 antibody directed against phospho-Ser2/-Ser5 within the heptad repeat at the C-terminus of the largest catalytic subunit of RNA polymerase II (a gift of H Kimura). Chromatin captured on magnetic beads was trimmed to create blunt ends, phosphate groups added to 5' ends, ends ligated to each other via biotinylated half-linkers, and complexes eluted. Crosslinks were then reversed, DNA purified and digested with *Mme*I (whose binding site is encoded by the linker). After immobilization on M-280 Streptavidin Dynabeads (Invitrogen), adaptors were ligated, and the efficiency of library production evaluated by PCR. Finally, di-tags were prepared, sequenced on a GAII analyzer (Illumina), and resulting paired-end tags (PETs) analysed. Libraries yielded $\sim 35 \times 10^6$ 20-bp paired-end reads each, from which 10.8×10^6 and 8.8×10^6 were successfully aligned to the genome (hg19) for the 0- and 30-min samples, respectively. For stringency, two or more reads having the same sequences, or mapping within 2 bp of the left and right ends of another read were classified as one PET; as a result most PETs were represented by many reads (for typical genome browser views, see Supplementary Figure S8B). PETs displayed some overlap to those seen by 4C as the two approaches carry different biases resulting from pull-down and amplification, respectively (e.g., in *SAMD4A* libraries ~13% of contacts are shared; Supplementary Figure S5B). For Figure 5C, genes were selected as follows. Sequences encoding

852 of the 1523 miRNAs in the database lie within 731 different RefSeq transcripts and 714 distinct genomic regions; PETs involving 701 and 703 of these regions (which we call 'miRNA genes') were seen in 0- and 30-min libraries. PETs/contacts seen between these miRNA genes, and between these miRNA genes and (i) an equal number of randomly selected genes, (ii) 916 and 921 genes at 0 and 30 min, respectively, that are the most highly expressed but non-induced ($<$1.5-fold), and (iii) 900 highly induced 30 min after stimulation ($>$1.9-fold) were then counted, and interaction frequencies (i.e., the number of PETs divided by the number of possible pairwise combinations expressed as a percentage) calculated.

Assessment of responsiveness to TNFα and SMAD binding

Responsiveness to TNFα was assessed using publicly available HUVEC microarray data (http://sbmdb.genome.rcast.u-tokyo.ac.jp/huvecdb/main_search.jsp); a gene was considered as responsive if mRNA levels increased $\geqslant$1.5-fold between 0 and 1 or 4 h after stimulation (average of all relevant probes in the database; 1 h after stimulation there are $\sim$500 responsive genes according to these criteria). SMAD binding was assessed using ChIP-chip and ChIP-seq data for SMAD1/5, and 2/3 from human keratinocytes (Koinuma *et al*, 2009a, b).

Analysis of miRNA targets

To assess functional relevance of miRNAs encoded by co-associating genes (by 4C and ChIA-PET), we selected from the HUVEC database the 100 most downregulated genes 1 or 4 h after TNFα stimulation; mRNA levels of these genes fell to between 2 and 42% of the 0-h level. Using default settings in the miRWalk database (Dweep *et al*, 2011), we queried how many mRNAs encoded by these 2×100 genes possessed (both predicted and experimentally validated) target sequences for the 24 miRNAs in their 3' untranslated regions. miR-711, -761, -3169, -3170, and -4293 were not included in the database, so a list of putative targets was generated using TargetScan (Lewis *et al,* 2005). Results are shown in Supplementary Table S4.

RNA FISH

RNA FISH was performed as described (Papantonis *et al*, 2010). Probes for *SAMD4A* intron 1, *EXT1* intron 1, and *EDN1* intron 2 were sets of five 50-mers; in each roughly every tenth thymine was tagged with Alexa 488 or 555. Probes were purified and labelled with an efficiency of 3.5–4.5 fluors/50-mer; *RCOR1* intron 1 was targeted by a set of 24 20-mers carrying one fluor each (Papantonis *et al*, 2010). Sets of multiplexed probes were four 55-mers (five internal amino-C6-modified thymines each, to which an average of four fluors was attached; IBA, Germany) targeting a $<$450 bp intronic region of seven genes shown to contact *SAMD4A*: *MYH9* (on HSA 22), *TNFAIP2*, *FBXO34*, *GCH1* (on 14), *LARP1B* (on 4), *ZNF608* (on 5), and *IL4R* (on 16). Precursors of miR-15a and -17 (on HSA 13), -155 (on 21), -105, -504, and -767 (on X), -191 and -425 (on 3), -1203 (on 17), and -1289-2 (on 5) were targeted by single 55-mers. These probes permit detection of single transcripts, which—when tested singly—never gave more than two foci (see also Wada *et al*, 2009 and Larkin *et al*, 2012), consistent with detection of nascent transcripts at both alleles. If additional (still-unspliced) transcripts were being detected, then we would expect to see additional foci. Note that the half-lives of segments within *SAMD4A* intron 1 are $\sim$5 min (e.g., Larkin *et al*, 2012). Note also that pairwise combinations of these probes yield colocalization frequencies comparable to those seen by others for co-transcribed genes (e.g., Brown *et al*, 2008; Schoenfelder *et al*, 2010). After DAPI staining, images were collected using an Axioplan 2 microscope (Zeiss) with a CoolSNAP$_{HQ}$ camera (Photometrics) via MetaMorph v. 7.1 (Molecular Devices). A focus is defined as $\geqslant$4 contiguous 90-nm pixels that contain signal above background (defined as the average intensity of a 50 pixel line-scan across the focus). Typically, FISH foci were 10 ± 3 pixels in size and deemed to colocalize if $\geqslant$25% red and green pixels overlapped.

Measurements of separations below the diffraction limit

The separation between peak intensities of overlapping foci was determined after identifying the position of each peak with 22-nm precision. Foci were identified manually and verified by a custom algorithm checking for: Gaussian shape and intensity above mean nuclear intensity plus 1 s.d. Next, the location of the emitter was estimated using the Joint Distribution algorithm (JD; Larkin and Cook, 2012). Pixel shift between fluorescence channels was corrected using 0.1-μm TetraSpeck beads (Molecular Probes) fluorescing at relevant wavelengths. Residual differences in alignment were accounted for along with spot intensity, shape, and signal-to-noise ratio to calculate uncertainty. Individual separation measurements and corresponding uncertainties were used to infer a probability distribution, which was compared to the model of a transcription factory (i.e., a 35-nm shell around a 90-nm core; Papantonis *et al*, 2010). All calculations were performed in MATLAB (MathWorks) using custom software routines.

Accession codes

ChIA-PET data are available in the Gene Expression Omnibus repository under accession number GSE41553.

Supplementary data

Supplementary data are available at *The EMBO Journal* Online (http://www.embojournal.org).

Acknowledgements

We thank Hiroshi Kimura for the Pd75C9 and Marc Vigneron for the 7C2 antibodies, Jon Bartlett for technical assistance, Shogo Yamamoto, Kaori Shiina, and Akashi Taguchi for help with deep sequencing. This work was supported by the Biotechnology and Biological Sciences Research Council and the ERASysBio+ initiative under the FP7/ERA-NET Plus scheme (AP), the Wellcome Trust (AP, JDL), the Felix Scholarship Trust of Oxford University (SB), the Medical Research Council (BD), the Japanese Society for the Promotion of Science through the Funding Program for World-Leading Innovative R&D on Science and Technology (TK), Grants-in-Aid for Scientific Research (B)22310117 (YW, TK) and Exploratory Research 23659050 (YW) from the Japanese Society for the Promotion of Science, and Scientific Research on Innovative Areas 23125503 (YW) from the Ministry of Education, Culture, Sports, Science and Technology, Japan.

Author contributions: AP, YW, TK, YR, and PRC conceived and designed experiments; AP prepared 4C libraries and did conventional sequencing, 3C, qRT–PCR, ChIP, blots, and RNA FISH; SB performed immuno-FISH and immunofluorescence; JDL developed and applied algorithms for high-resolution and NN analyses; BD isolated factory fractions; YK, MK, HA, and YW did ChIP-seq, 'deep'-sequenced 4C libraries, and prepared ChIA-PET templates; GL, HMP, XR, and YR performed ChIA-PET and analysed the resulting data; ST, TK, and GL generated high-throughput data sets and mined ChIA-PET data; ST provided help with bioinformatics and generated Circos diagrams; PS did the statistical analysis for the number of NFκB factories; AP, YW, TK, YR, GL, and PRC analysed the data and wrote the manuscript.

Conflict of interest

The authors declare that they have no conflict of interest.

References

Apostolou E, Thanos D (2008) Virus Infection Induces NF-kappaB-dependent interchromosomal associations mediating monoallelic IFN-beta gene expression. *Cell* **134:** 85–96

Ashall L, Horton CA, Nelson DE, Paszek P, Harper CV, Sillitoe K, Ryan S, Spiller DG, Unitt JF, Broomhead DS, Kell DB, Rand DA, Sée V, White MR (2009) Pulsatile stimulation determines timing and specificity of NF-kappaB-dependent transcription. *Science* **324:** 242–246

Brown JM, Green J, das Neves RP, Wallace HA, Smith AJ, Hughes J, Gray N, Taylor S, Wood WG, Higgs DR, Iborra FJ, Buckle VJ (2008)

Association between active genes occurs at nuclear speckles and is modulated by chromatin environment. *J Cell Biol* **182:** 1083–1097

Cai S, Lee CC, Kohwi-Shigematsu T (2006) SATB1 packages densely looped transcriptionally active chromatin for coordinated expression of cytokine genes. *Nat Genet* **38:** 1278–1288

Chakalova L, Fraser P (2010) Organization of transcription. *Cold Spring Harb Perspect Biol* **2:** a000729

Chubb JR, Liverpool TB (2010) Bursts and pulses: insights from single cell studies into transcriptional mechanisms. *Curr Opin Genet Dev* **20:** 478–484

Cook PR (2010) A model for all genomes; the role of transcription factories. *J Mol Biol* **395:** 1–10

Dekker J, Rippe K, Dekker M, Kleckner N (2002) Capturing chromosome conformation. *Science* **295:** 1306–1311

de Wit E, de Laat W (2012) A decade of 3C technologies: insights into nuclear organization. *Genes Dev* **26:** 11–24

Dhar SS, Wong-Riley MTT (2010) Chromosome conformation capture of transcriptional interactions between cytochrome c oxidase genes and genes of glutamatergic synaptic transmission in neurons. *J Neurochem* **115:** 676–683

Dweep H, Sticht C, Pandey P, Gretz N (2011) miRWalk - Database: Prediction of possible miRNA binding sites by ''walking'' the genes of three genomes. *J Biomed Inform* **44:** 839–847

Eskiw CH, Rapp A, Carter DR, Cook PR (2008) RNA polymerase II activity is located on the surface of ~87 nm protein-rich transcription factories. *J Cell Sci* **121:** 1999–2007

Ethier SD, Miura H, Dostie J (2012) Discovering genome regulation with 3C and 3C-related technologies. *Biochim Biophys Acta* **1819:** 401–410

Ferrai C, Xie SQ, Luraghi P, Munari D, Ramirez F, Branco MR, Pombo A, Crippa MP (2010) Poised transcription factories prime silent uPA gene prior to activation. *PLoS Biol* **8:** e1000270

Fullwood MJ, Liu MH, Pan YF, Liu J, Xu H, Mohamed YB, Orlov YL, Velkov S, Ho A, Mei PH, Chew EG, Huang PY, Welboren WJ, Han Y, Ooi HS, Ariyaratne PN, Vega VB, Luo Y, Tan PY, Choy PY *et al* (2009) An oestrogen-receptor-alpha-bound human chromatin interactome. *Nature* **462:** 58–64

Göndör A, Ohlsson R (2009) Chromosome crosstalk in three dimensions. *Nature* **461:** 212–217

Göndör A, Rougier C, Ohlsson R (2008) High-resolution circular chromosome conformation capture assay. *Nat Protoc* **3:** 303–313

Grøntved L, Hager GL (2012) Impact of chromatin structure on PR signaling: Transition from local to global analysis. *Mol Cell Endocrinol* **357:** 30–36

Guo H, Ingolia NT, Weissman JS, Bartel DP (2010) Mammalian microRNAs predominantly act to decrease target mRNA levels. *Nature* **466:** 835–840

Hall LL, Smith KP, Byron M, Lawrence JB (2006) Molecular anatomy of a speckle. *Anat Rec A Discov Mol Cell Evol Biol* **288:** 664–675

Koinuma D, Tsutsumi S, Kamimura N, Imamura T, Aburatani H, Miyazono K (2009a) Promoter-wide analysis of Smad4 binding sites in human epithelial cells. *Cancer Sci* **100:** 2133–2142

Koinuma D, Tsutsumi S, Kamimura N, Taniguchi H, Miyazawa K, Sunamura M, Imamura T, Miyazono K, Aburatani H (2009b) Chromatin immunoprecipitation on microarray analysis of Smad2/3 binding sites reveals roles of ETS1 and TFAP2A in transforming growth factor beta signaling. *Mol Cell Biol* **29:** 172–186

Kolovos P, Knoch TA, Grosveld FG, Cook PR, Papantonis A (2012) Enhancers and silencers: an integrated and simple model for their function. *Epigenetics Chromatin* **5:** 1

Larkin JD, Cook PR (2012) Maximum precision closed-form solution for localizing diffraction-limited spots in noisy images. *Opt Express* **20:** 18478–18493

Larkin JD, Cook PR, Papantonis A (2012) Dynamic reconfiguration of long human genes during one transcription cycle. *Mol Cell Biol* **32:** 2738–2747

Lewis BP, Burge CB, Bartel DP (2005) Conserved seed pairing often flanked by adenosines indicates that thousands of human genes are microRNA targets. *Cell* **120:** 15–20

Li G, Fullwood MJ, Xu H, Mulawadi FH, Velkov S, Vega V, Ariyaratne PN, Mohamed YB, Ooi HS, Tennakoon C, Wei CL, Ruan Y, Sung WK (2010) ChIA-PET tool for comprehensive chromatin interaction analysis with paired-end tag sequencing. *Genome Biol* **11:** R22

Li G, Ruan X, Auerbach RK, Sandhu KS, Zheng M, Wang P, Poh HM, Goh Y, Lim J, Zhang J, Sim HS, Peh SQ, Mulawadi FH, Ong CT, Orlov YL, Hong S, Zhang Z, Landt S, Raha D, Euskirchen G *et al* (2012) Extensive promoter-centered chromatin interactions provide a topological basis for transcription regulation. *Cell* **148:** 84–98

Lieberman-Aiden E, van Berkum NL, Williams L, Imakaev M, Ragoczy T, Telling A, Amit I, Lajoie BR, Sabo PJ, Dorschner MO, Sandstrom R, Bernstein B, Bender MA, Groudine M, Gnirke A, Stamatoyannopoulos J, Mirny LA, Lander ES, Dekker J (2009) Comprehensive mapping of long-range interactions reveals folding principles of the human genome. *Science* **326:** 289–293

Lomvardas S, Barnea G, Pisapia DJ, Mendelsohn M, Kirkland J, Axel R (2006) Interchromosomal interactions and olfactory receptor choice. *Cell* **126:** 403–413

Melnik S, Deng B, Papantonis A, Baboo S, Carr IM, Cook PR (2011) The proteomes of transcription factories containing RNA polymerases I II or III. *Nat Methods* **8:** 962–968

Meulmeeste E, Ten Dijke P (2011) The dynamic roles of TGF-β in cancer. *J Pathol* **223:** 205–218

Mitchell JA, Fraser P (2008) Transcription factories are nuclear subcompartments that remain in the absence of transcription. *Genes Dev* **22:** 20–25

Morlando M, Ballarino M, Gromak N, Pagano F, Bozzoni I, Proudfoot NJ (2008) Primary microRNA transcripts are processed co-transcriptionally. *Nat Struct Mol Biol* **15:** 902–909

Nechaev S, Adelman K (2008) Promoter-proximal Pol II: when stalling speeds things up. *Cell Cycle* **7:** 1539–1544

Noordermeer D, Leleu M, Splinter E, Rougemont J, De Laat W, Duboule D (2011a) The dynamic architecture of Hox gene clusters. *Science* **334:** 222–225

Noordermeer D, de Wit E, Klous P, van de Werken H, Simonis M, Lopez-Jones M, Eussen B, de Klein A, Singer RH, de Laat W (2011b) Variegated gene expression caused by cell-specific long-range DNA interactions. *Nat Cell Biol* **13:** 944–951

Osborne CS, Chakalova L, Brown KE, Carter D, Horton A, Debrand E, Goyenechea B, Mitchell JA, Lopes S, Reik W, Fraser P (2004) Active genes dynamically colocalize to shared sites of ongoing transcription. *Nat Genet* **36:** 1065–1071

Papantonis A, Larkin JD, Wada Y, Ohta Y, Ihara S, Kodama T, Cook PR (2010) Active RNA polymerases: mobile or immobile molecular machines? *PLoS Biol* **8:** e1000419

Pawlicki JM, Steitz JA (2008) Primary microRNA transcript retention at sites of transcription leads to enhanced microRNA production. *J Cell Biol* **182:** 61–76

Pierce JW, Schoenleber R, Jesmok G, Best J, Moore SA, Collins T, Gerritsen ME (1997) Novel inhibitors of cytokine-induced IkappaB-alpha phosphorylation and endothelial cell adhesion molecule expression show anti-inflammatory effects in vivo. *J Biol Chem* **272:** 21096–21103

Pombo A, Cook PR (1996) The localization of sites containing nascent RNA and splicing factors. *Exp Cell Res* **229:** 201–203

Pombo A, Jackson DA, Hollinshead M, Wang Z, Roeder RG, Cook PR (1999) Regional specialization in human nuclei: visualization of discrete sites of transcription by RNA polymerase III. *EMBO J* **18:** 2241–2253

Robyr D, Friedli M, Gehrig C, Arcangeli M, Marin M, Guipponi M, Farinelli L, Barde I, Verp S, Trono D, Antonarakis SE (2011) Chromosome conformation capture uncovers potential genome-wide interactions between human conserved non-coding sequences. *PLoS ONE* **6:** e17634

Schoenfelder S, Sexton T, Chakalova L, Cope NF, Horton A, Andrews S, Kurukuti S, Mitchell JA, Umlauf D, Dimitrova DS, Eskiw CH, Luo Y, Wei CL, Ruan Y, Bieker JJ, Fraser P (2010) Preferential associations between co-regulated genes reveal a transcriptional interactome in erythroid cells. *Nat Genet* **42:** 53–61

Simonis M, Klous P, Splinter E, Moshkin Y, Willemsen R, de Wit E, van Steensel B, de Laat W (2006) Nuclear organization of active and inactive chromatin domains uncovered by chromosome conformation capture-on-chip 4C. *Nat Genet* **38:** 1348–1354

Smale ST (2010) Selective transcription in response to an inflammatory stimulus. *Cell* **140:** 833–844

Soler E, Andrieu-Soler C, de Boer E, Bryne JC, Thongjuea S, Stadhouders R, Palstra RJ, Stevens M, Kockx C, van Ijcken W,

Hou J, Steinhoff C, Rijkers E, Lenhard B, Grosveld F (2010) The genome-wide dynamics of the binding of Ldb1 complexes during erythroid differentiation. *Genes Dev* **24:** 277–289

Spector DL, Lamond AI (2011) Nuclear speckles. *Cold Spring Harb Perspect Biol* **3:** a000646

Suárez Y, Fernández-Hernando C, Yu J, Gerber SA, Harrison KD, Pober JS, Iruela-Arispe ML, Merkenschlager M, Sessa WC (2008) Dicer-dependent endothelial microRNAs are necessary for postnatal angiogenesis. *Proc Natl Acad Sci USA* **105:** 14082–14087

Suárez Y, Wang C, Manes TD, Pober JS (2010) Cutting edge: TNF-induced microRNAs regulate TNF-induced expression of E-selectin and intercellular adhesion molecule-1 on human endothelial cells: feedback control of inflammation. *J Immunol* **184:** 21–25

Sullivan DE, Ferris M, Nguyen H, Abboud E, Brody AR (2009) TNF-alpha induces TGF-beta1 expression in lung fibroblasts at the transcriptional level via AP-1 activation. *J Cell Mol Med* **13:** 1866–1876

Wada Y, Ohta Y, Xu M, Tsutsumi S, Minami T, Inoue K, Komura D, Kitakami J, Oshida N, Papantonis A, Izumi A, Kobayashi M, Meguro H, Kanki Y, Mimura I, Yamamoto K, Mataki C, Hamakubo T, Shirahige K, Aburatani H *et al* (2009) A wave of nascent transcription on activated human genes. *Proc Natl Acad Sci USA* **106:** 18357–18361

Würtele H, Chartrand P (2006) Genome-wide scanning of HoxB1-associated loci in mouse ES cells using an open-ended chromosome conformation capture methodology. *Chromosome Res* **14:** 477–495

Xu M, Cook PR (2008) Similar active genes cluster in specialized transcription factories. *J Cell Biol* **181:** 615–623

Yaffe E, Tanay A (2011) Probabilistic modeling of Hi-C contact maps eliminates systematic biases to characterize global chromosomal architecture. *Nat Genet* **43:** 1059–1065

Zentner GE, Tesar PJ, Scacheri PC (2011) Epigenetic signatures distinguish multiple classes of enhancers with distinct cellular functions. *Genome Res* **21:** 1273–1283

Zhao Z, Tavoosidana G, Sjölinder M, Göndör A, Mariano P, Wang S, Kanduri C, Lezcano M, Sandhu KS, Singh U, Pant V, Tiwari V, Kurukuti S, Ohlsson R (2006) Circular chromosome conformation capture 4C uncovers extensive networks of epigenetically regulated intra- and interchromosomal interactions. *Nat Genet* **38:** 1341–1347

Supplementary data

Papantonis *et al* (2012) TNFα signals through specialized factories where responsive coding and miRNA genes are transcribed

This section contains:

—Supplementary Methods and References

—Supplementary Figures S1-S8 and their respective legends

—Legends to Supplementary Tables S1-S7 (Tables provided separately as an .xls file)

Supplementary Methods

Oligonucleotides

Oligonucleotides were designed to be 20-22 nt-long, have a T*m* of 62°C, and yield amplimers of 75-225 bp using Primer 3.0 Plus (http://www.bioinformatics.nl/cgi-bin/primer3plus /primer3plus.cgi). For 4C libraries prepared using *Sac*I, primer sequences used for nested inverse PCR on fragments spanning the TSS of our reference genes were (ExF—external forward primer; InF—internal forward primer; ExR—external reverse primer; InR—internal reverse primer):

(i) For *SAMD4A*:

(Sac-ExF) ACATTGAGGGAGATTCCATTGAG,

(Sac-ExR) TGAAGACGAAGCTCTAAAACCAGA,

(Sac-InF) TTCCTCCTCCCTAGTATGGTGTG,

(Sac-InR) AAGTAACCCACTTCATGCCTGTC.

(ii) For *EXT1* (semi-nested PCR):

(Sac-ExF/InF) CTAGAGGCTGGGGACAGAGAGTT,

(Sac-InR) CAAAGTTGGGTCGGAAGTTTTC,

(Sac-ExR) TGGGATGATCCTTAGAAAAGAGG.

For libraries prepared using *Hind*III, they were:

(i) For *SAMD4A*:

(Hind-ExF) ATATCCGGAAACTAGCCAAGAAC,

(Hind-ExR) ACGCTAGCAAATAGGAAACTCGT,

(Hind-InF) GAGAATATTTCAGGCCCTCTCTCA,

(Hind-InR) AAGTAACCCACTTCATGCCTGTC.

(ii) For *EXT1*:

(Hind-ExF) CCACCAAGAGAATAACATCACTTTG,

(Hind-ExR) CCAACTGTCCCAGCTATAGAAG,

(Hind-InF) ATCTTTAACACCACCACCACCAC,

(Hind-InR) AAGGACATATGACTGGTAGAATTGC.

(iii) For *ETS2*:

(ExF) ATACAATGGAAGCGCCTGTG,

(ExR) TCTCCAAAGGGGACTGCTC,

(InF) GTTATCTGCCTGCCCACAC,

(InR) TAGCGCGTCAACTACTGTTTTAG.

All other primer sequences are available on request.

Chromatin immunoprecipitation (ChIP)

For p65 ChIP followed by quantitative PCR, ~10^7 HUVECs were cross-linked (10 min; 20°C) in 1% paraformaldehyde and chromatin was prepared using the ChIP-IT-Express kit (Active motif). Immunoprecipitations were performed using a polyclonal antibody against the p65 subunit of NFκB (4 µg/reaction; sc-372X, Santa Cruz Biotechnology) or against the N-terminus of the largest subunit of RNA polymerase II (2 µg/reaction; sc-889X, Santa Cruz Biotechnology). DNA was purified using a MicroElute Cycle-Pure kit prior to quantitative real-time PCR (Platinum SYBR Green qPCR Mix-UDG, Invitrogen). Reactions were 50°C/2 min, 95°C/5 min, and 40 cycles at 95°C/15 sec, and 60°C/50 sec. Data was analyzed (Nelson *et al,* 2006) using the *TNFAIP3* promoter (for p65 binding) and *GAPDH* TATA box (for RNAPII binding) as positive, and the *AFP* 3' UTR as a negative control.

For p65 ChIP followed by next-generation sequencing, cells were crosslinked as for ChIA-PET, sonicated (Branson sonicator 250, 10 min), and immunoprecipitation performed using an anti-p65 polyclonal antibody (Abcam, ab7970) and Protein A-coated magnetic beads (Dynal). DNA bound to beads was isolated, and enrichment evaluated by qPCR using primers targeting promoters of genes known to bind p65 (*TNFAIP3* and *CXCL1*). Primer sequences were: TNFAIP3F—CTGGGAGTTTGTT GGACGTT, TNFAIP3R—AACCTCTGCAGCAGTGACCT; CXCL1F—AGGGAATTCACCCCAAGAAC, CXCL1R—GGCGGGACTTACATGACTTC. From ~13 x 10^6 36-bp reads (for each of the 0 and 30 min datasets), ~8 x 10^6 uniquely mapped t the genome (hg18). These were clustered into >12,000 p65-binding sites (consistent with results of Kasowski *et al*, 2009), and it is now known that NFκB binds to many sites scattered around the genome, including *Alu* repeats (Antonaki *et al*, 2011).

ChIP for RNA polymerase II and histone modifications was carried out as described (Wada *et al,* 2009), and coupled to next-generation sequencing. Briefly, 2x10^6 HUVEC cells were grown, serum-starved, stimulated with TNFα for 30 min, cross-linked using 1% paraformaldehyde (10 min; 20°C), neutralized in 0.2 M glycine/PBS, lyzed in 10 mM Tris-HCl (pH 8.0), 150 mM NaCl, 1% SDS, plus 1mM EDTA, and DNA sonicated to ~300 bp. RNA polymerase II-bound chromatin was pulled down using the mouse monoclonal antibody Pd75C9 (as above). After purification, DNA was sequenced, reads mapped as for 4C-seq and extended to 200 bp. Clusters containing significantly more reads were identified by comparison to a Poissonian background model (P <10^{-9}). A gene was considered able to bind polymerase if a peak >5-fold higher than background was detected between -3 to +1 kbp of the transcription start site. From ~20 x 10^6 36-bp reads (for each of the 0 and 30 min datasets), ~14 x 10^6 were uniquely mapped against the genome (hg18). ChIP-seq data are available at the GEO database (NCBI) under accession number GSE34500. Views shown in **Supplementary Figures S2E**, **S3C**, and **S8** were obtained using the Integrated Genome Browser (IGB) v 6.4.

Quantitative reverse transcriptase PCR (qRT-PCR)

Total RNA was isolated using TRIzol (Invitrogen) from 10^7 cells stimulated with TNFα (0-60 min), treated with RQ1 DNase (1 unit of DNase/μg of total RNA; 37°C for 45 min; Promega), and nascent RNA amplified (54°C/10 min followed by 1 cycle at 95°C/5 min, 40 cycles of 95°C/15 sec, 60°C/50 sec, and a single cycle at 40°C/2 min; Rotor-Gene 3000 cycler, Corbett) using the One-Step qRT-PCR kit (Invitrogen) with primers targeting introns. The presence of single amplimers was confirmed by melting curve analysis. Reactions in which Platinum *Taq* polymerase (Invitrogen) replaced the RTase/*Taq* polymerase mix were performed to ensure amplimers did not result from residual genomic DNA. Precursor and mature miRNAs were detected using miScript assays (Qiagen) with levels normalized relative to mature RNU6.

Immunofluorescence (IF)

HUVECs grown on coverslips etched with hydrofluoric acid were fixed with 4% paraformaldehyde (Electron Microscopy Science) in 250 mM HEPES (pH 7.6; 20 min; 20°C), washed 3x in PBS (5 min; 20°C), permeabilized using 0.5% Triton X-100/0.5% saponin in PBS (20 min; 20°C), washed with 0.05% Tween 20 in PBS (10 min; 20°C), and blocked with 3% BSA/0.2% gelatin in PBS (Sigma; 20 min; 20°C). Phosphorylated (at Ser536) p65 was detected using a rabbit monoclonal antibody (1:1,000 dilution; #3033, Cell Signalling Technology) and Alexa488- or Cy3-conjugated donkey anti-rabbit IgG (0.5 μg/ml; Invitrogen). After DAPI counter-staining, images were collected as for RNA FISH and analysed using ImageJ (Abramoff *et al,* 2004); an area of 1292x1292 pixels was arbitrarily selected in the nucleus, the mean intensity calculated, and nuclear fluorescence (arbitrary units, au) calculated by subtracting the background (measured as the minimum intensity in the area).

Immunofluorescence and fluorescence in situ hybridization (Immuno-FISH)

HUVECs on coverslips were fixed and washed as above, stored in 70% ethanol (4°C; 48 h), transferred to PBS (5 min; 20°C), permeabilized with 0.5% Triton X-100/0.5% saponin in PBS (20 min; 20°C), rinsed in water, post-fixed with 4% paraformaldehyde in PBS (5 min; 20°C), washed in PBS (10 min; 20°C), gradually dehydrated in ethanol (70%, 90% and 100%), and allowed to hybridize (16 h; 37°C) with 25 ng (for *SAMD4A* and *EXT1*) or 10 ng (for *EDN1*) of the relevant probes in hybridization mix (25% deionized formamide, 2x SSC, 200 ng/μl sheared salmon sperm DNA, 5x Denhardt's, 50 mM phosphate buffer, 1 mM EDTA, 0.5 μl murine RNase inhibitor). RNA FISH probes were the sets of five 50-mers described above. Next day, coverslips were washed 3x in 2xSSC (10 min; 37°C), processed for immunofluorescence, and imaged as described above. For the panel in **Supplementary Figure S5D** illustrating non-colocalization of nascent *EDN1* RNA and $p65^P$ (detected using Alexa 488 and Cy3, respectively), the red channel is pseudo-colored green, and the green

channel pseudo-colored red (to facilitate comparison with the other panels). A (red) FISH focus (defined as above) was deemed to colocalize with a (green) p65 focus if ≥33% of red pixels overlapped green pixels.

BrUTP labeling, immunofluorescence, and nearest-neighbour analysis

HUVECs on coverslips were induced with TNFα, washed in ice-cold PB+ (100 mM CH_3COOK, 30 mM KCl, 10 mM Na_2HPO_4, 1 mM $MgCl_2$, 10 mM NaF, 10 mM β-glycerophosphate, 200 μM Na_3VO_4, 1 mM Na_2ATP, 1 mM DTT, 1:1000 PIC, 1:2000 RNaseOUT; pH 7.6) for 1 min, permeabilized in 170 μg/ml saponin (Sigma)/PB+ for 5 min on ice, washed 3x in ice-cold PB+, incubated (5 min; 33˚C) in transcription buffer (PB+ with 100 μM each of ATP, GTP and CTP, 100 μM $MgCl_2$, 1:100 RNaseOUT), 100 μM BrUTP (Sigma) added and a "run-on" carried out (15 min; 33˚C), and stopped by adding 2.5 mM EDTA (pH 8.0). Then, cells were washed 2x in ice-cold PB+, fixed in 4% PFA/250 mM HEPES (20 min; room temperature), washed 3x in PBS (5 min; room temperature), and prepared for immunofluorescence, imaged, and images aligned as for high-resolution RNA FISH. Primary antibodies were: (i) rabbit monoclonal against phosphorylated (Ser 536) p65 (1:1000 dilution; Cell Signaling Technology), and (ii) mouse monoclonal against BrUTP (1:1000 dilution; Phoenix Flow Systems). Secondary antibodies were: (i) Alexa488-conjugated donkey anti-rabbit IgG (0.5 μg/ml; Invitrogen), and (ii) DyLight649-conjugated donkey anti-mouse IgG (7 μg/ml; Jackson ImmunoResearch). For "nearest-neighbour" (NN) analysis, foci were identified automatically as follows. The nuclear region was selected (using a threshold in the DAPI image), foci with Gaussian shape selected independently of intensity, features too small to represent true foci removed (*i.e.*, ≤4 pixels in a 2x2 array), and foci selected in which the brightest pixel had an intensity greater than both the average global background (*i.e.*, the mean nuclear intensity plus half a SD) and the average local background (measured in the 43 outermost pixels in the 9x9 array around the brightest pixel); >90% foci seen by eye survived this selection. Then, peak intensities within the selected foci were localized with 22-nm precision using the "tuned" version of the JD algorithm (Larkin and Cook, 2012), and the distance from the peak of each red (or green) focus to its closest (in 2D space) green (or red) focus was determined. A total of 2865 foci from 8 nuclei were analyzed. As a control, 8243 randomly-distributed foci with the same density were computer-generated. All calculations were performed in MATLAB (MathWorks) using custom software routines available on request.

Association of $p65^P$ with large fragments of transcription factories

Here, a method for isolating large fragments of factories of >8 MDa was followed exactly (Melnik *et al,* 2011). HUVECs were treated with TNFα for 0 or 15 min, nuclei isolated in PB+ buffer (see above),

and most chromatin detached from the nuclear sub-structure using DNase I; after spinning, the supernatant (*i.e.*, fraction "4super") contains chromatin. The pellet was resuspended, treated with caspases, and respun; the supernatant (*i.e.*, fraction "5super") contains large fragments of factories. The two supernatants containing either "chromatin" or large fragments of "factories" were then resolved by SDS-PAGE electrophoresis in 10% acrylamide gels (Bio-Rad), proteins transferred onto nitrocellulose using the iBlot Transfer System (Invitrogen), and phospho-p65 ($p65^{P}$), RCC1 (a negative control), and RNA polymerase II detected by immuno-blotting using the rabbit monoclonal antibody (1:3,000 dilution; #3033, Cell Signalling Technology), a mouse monoclonal anti-RCC1 (1:3,000 dilution; R35420, Transduction Laboratories), and a mouse monoclonal anti-RPB1 (7C2; 1:10,000 dilution; a gift of Marc Vigneron), respectively.

DNA fluorescence in situ hybridization (DNA FISH)

DNA FISH was performed as described (Li *et al*, 2012). In brief, HUVECs grown on coverslips were stimulated with TNFα for 30 min, fixed in 3:1 methanol/acetic acid (15 min; room temperature), washed 3x in PBS, and stored in 70% ethanol at -20°C. Then, cells were washed once in PBS, once in 100 mM Tris-HCl (pH 7.5) plus 150 mM NaCl, digested with pepsin/HCl (5 min; 37°C; as for RNA FISH), rinsed in water, post-fixed in 1% PFA/PBS (5 min; room temperature), washed 2x in PBS, dehydrated via a 70%-90%-100% ethanol series, and chromatin denatured in 2x SSC/60% formamide (40 min; 80°C). Meanwhile, probes were denatured (10 min; 90°C) in hybridization buffer (as for RNA FISH, but with 50% formamide), quenched on ice, added to cells, coverslips sealed on to slides using rubber cement (Fixogum, Marabu), and hybridized in a moist chamber (37°C; 24 h). Next day, slides were washed twice in 2x SSC (5 min; 37°C) to remove coverslips, which were in turn washed 3x in 2x SSC (10 min; 37°C), mounted on to new slides, and imaged as for RNA FISH. Probes were produced from BAC clones (CTD-2589I5 for *SAMD4A*, RP11-720F6 for *SLC6A5*, and RP11-194M2 for *EDN1*; all from CHORI) nick-translated and conjugated to Alexa 488 or 555 using the FISH-Tag kit (Invitrogen). Genomic loci were considered as colocalizing when >10% of pixels in the respective FISH foci overlapped; ~100 cells per probe pair were analyzed.

Estimating numbers of "NFκB" factories

After stimulation our reference genes share few contacts (**Supplementary Figure S7**, and **Tables S1** and **S2**), and RNA FISH using multiplexed probes reveals that most nascent targets do not colocalize with each other. We estimate that ~8 "NFκB" factories are accessible to *SAMD4A* and to each of the 7 other responsive genes analyzed in **Figure 4A** as follows: the probability, *P*, that at least one of the 7 nascent transcripts colocalizes with a nascent *SAMD4A* transcript is given by $1-[(n-1)/n]^{7}$, where *n* is the number of "NFκB" factories that all 8 genes can access at a high frequency; as $P = 0.6$ (**Figure**

4A), *n* = 8. That a gene like *SAMD4A* can access ~8 "NFκB" factories is consistent with the fact that 30 min after stimulation (in nuclei containing at least one green and one red focus) ~8% nascent *SAMD4A* transcripts colocalize with nascent RNA copied from one gene in the multiplexed set, *TNFAIP2* (Papantonis *et al*, 2010). If both can access the same 8 "NFκB" factories with equal chance, the probability that a nascent *TNFAIP2* transcript is found in a factory already containing a *SAMD4A* transcript is 1/8 or 12% (comparable to the 8% seen experimentally). The total number of polymerase II factories in the (G0) HUVEC nucleoplasm is ~2,200 assuming: (i) the density of factories in the HUVEC nucleoplasm is the same as in several other mammalian cells—~9.3 factories/μm^3 (Faro-Trindade and Cook, 2006; densities corrected for a revised factory diameter of 87 nm; Eskiw *et al*, 2008), (ii) the nuclear volume of HUVECs is 300 ± 87 μm^3 (*n* = 15; measured by confocal microscopy of fixed, DAPI-stained nuclei), and (iii) non-nucleolar volume occupies 80% nuclear volume (*i.e*., in the middle of the range seen in other mammalian cells; Faro-Trindade and Cook, 2006). The number of "NFκB" factories will be a fraction of the above, and we can place an upper bound on it in two ways. First, using RNA FISH data; 31% yellow foci (*i.e*., 60%-29%=31%; see **Supplementary Figure S5A**) are then expected using probes targeting *SAMD4A* and 3 multiplexed targets encoded by the same chromosome as *SAMD4A*. Using the same equation as above, *P* is then 0.31, thus *n*=8. If all responsive genes on chromosome 14 (which represents 2.5% of the genome) can access the same ~8 "NFκB" factories, and if the number of "NFκB" factories scales with amount of DNA, there will be 320 "NFκB" factories. This is an upper estimate, as responsive genes on different chromosomes clearly share "NFκB" factories. Second, using ChIA-PET data; we select 606 genes that are up-regulated >3-fold between 0 and 30 min (using contact frequencies, as these accurately reflect transcriptional activity; Li *et al*, 2012). 496 genes in this set contact at least one other member in the set (6,266 interactions in total). If these 496 genes access essentially all "NFκB" factories, successively removing the gene making the fewest contacts from the set, then the next fewest, and so on, should initially have little effect on the total number of interactions; this is the case (**Supplementary Figure S6D**; data for other sets of genes are included for comparison). Then, when too few up-regulated genes in the set remain to saturate all "NFκB" factories with contacts, the number of interactions should begin to fall; this number is ~250 and this is also an upper limit of the number of "NFκB" factories. These values are consistent with ~150 $p65^P$ foci per nucleus (**Supplementary Figure S5D**); if such foci mark most "NFκB" factories, there might be ~150-250 such factories. Note that the estimates given here are inevitably coarse ones, given the number of assumptions.

Statistical analysis

P values (two-tailed) from Fisher's exact test, Chi-square test with Yates' correction, and unpaired Student's *t*-test were calculated using GraphPad (http://www.graphpad.com); they were considered significant when <0.05. Pearson's correlation coefficient (*R*) was calculated using Excel (Microsoft). *P* values from the binomial distribution and Kolmogorov-Smirnov two-sample tests (in **Supplementary Figures S4** and **S5**, respectively) were calculated manually.

Supplementary references

Abramoff MD, Magelhaes PJ, Ram SJ (2004) Image processing with ImageJ. *Biophot Int* **11**: 36-42

Antonaki A, Demetriades C, Polyzos A, Banos A, Vatsellas G, Lavigne MD, Apostolou E, Mantouvalou E, Papadopoulou D, Mosialos G, Thanos D (2011) Genomic analysis reveals a novel nuclear factor-κB (NF-κB)-binding site in Alu-repetitive elements. *J Biol Chem* **286**: 38768-38782

Faro-Trindade I, Cook PR (2006) A conserved organization of transcription during embryonic stem cell differentiation and in cells with high C value. *Mol Biol Cell* **17**: 2910-2920

Kasowski M, Grubert F, Heffelfinger C, Hariharan M, Asabere A, Waszak SM, Habegger L, Rozowsky J, Shi M, Urban AE, Hong MY, Karczewski KJ, Huber W, Weissman SM, Gerstein MB, Korbel JO, Snyder M (2010) Variation in transcription factor binding among humans. *Science* **328**: 232-235

Krzywinski M, Schein J, Birol I, Connors J, Gascoyne R, Horsman D, Jones SJ, Marra MA (2009) Circos: An information aesthetic for comparative genomics. *Genome Res* **19**: 1639-1645

Nelson JD, Denisenko O, Bomsztyk K (2006) Protocol for the fast chromatin immunoprecipitation ChIP method. *Nat Protoc* **1**: 179-185

Supplementary Figure S1

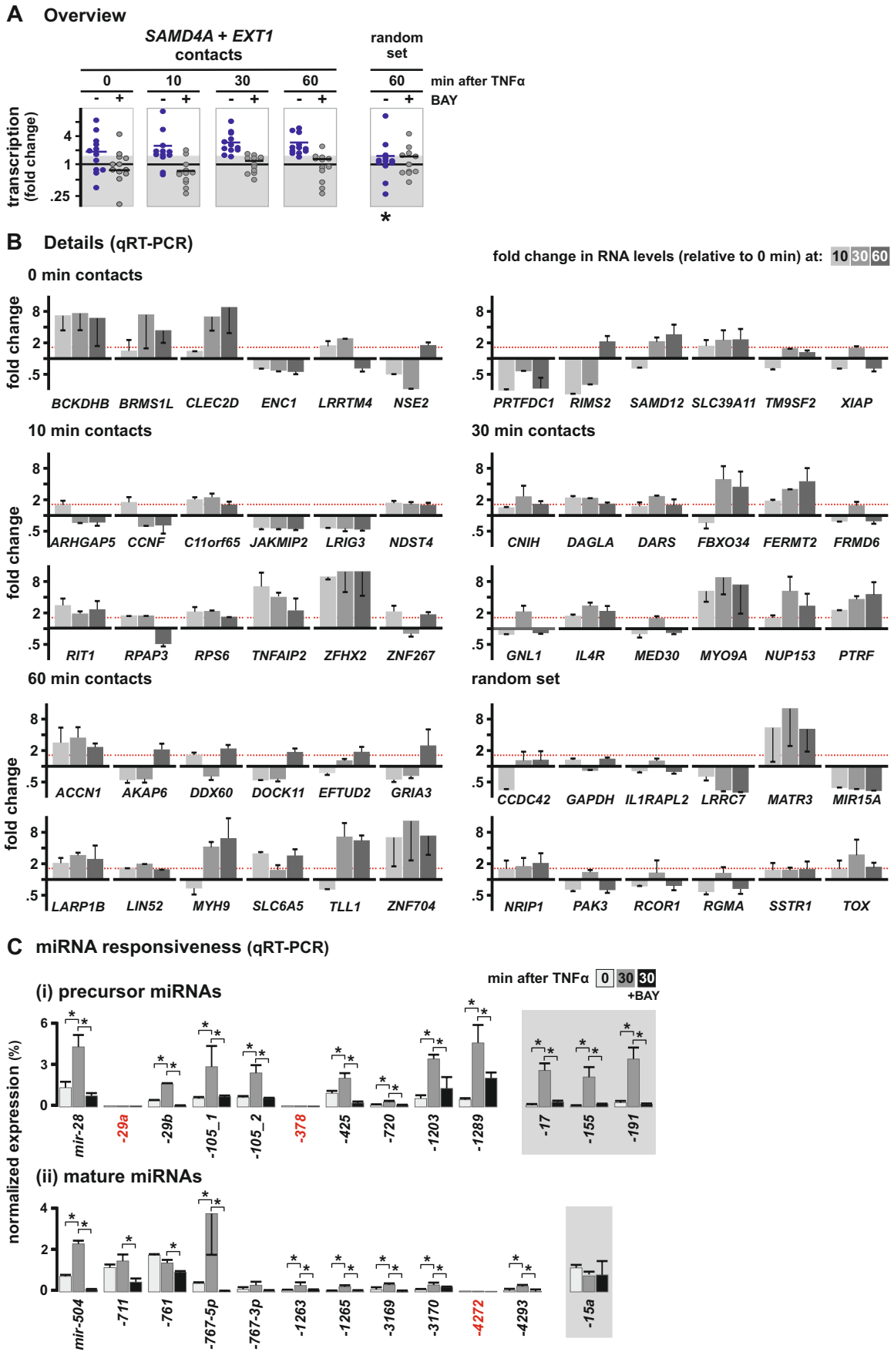

Supplementary Figure S1 Quantitative RT-PCR shows that most contacted coding and non-coding genes respond to TNFα. HUVECs were grown ±BAY for 1 h, treated with TNFα for up to 60 min, and relative levels of nascent transcripts assessed using qRT-PCR with intronic probes. (**A**) Overview of results for a set of 12 genes contacted by *SAMD4A* and *EXT1* at 0-60 min after stimulation (genes selected at random from the set of all those contacted); a set of randomly-selected human genes provides a control. Circles indicate fold-change relative to 0-min value (for 0-min contacts, the respective 60-min values are used) and black lines give mean. Genes in each experimental set were significantly up-regulated, compared to the random set (1.5-fold threshold indicated by grey shading). BAY abolished this up-regulation (grey circles). *: $P<0.01$ ($n=4$; unpaired two-tailed Student's *t*-test). (**B**) Details for the genes analyzed in (A). Changes in nascent RNA levels (relative to 0-min level; ± SD; $n=4$) are shown for each gene. No more than 3 genes in the random set are up-regulated >1.5-fold (red dotted line) at any time-point. In contrast, significantly more genes in each of the experimental sets were up-regulated at the relevant time ($P=0.0375$, 0.003, 0.01, and 0.003 for the 0-, 10-, 30-, and 60-min sets, respectively; two-tailed Fisher's exact test). (**C**) A similar analysis of (**i**) pre-miRNAs and (**ii**) mature miRNAs. Pre- and mature miRNAs were chosen because their host genes were contacted 30 min after stimulation by *MIR17HG*, *MIR155HG*, or *MIR191* (in 4C or ChIA-PET libraries). Levels are expressed as a percentage of those of RNU6 RNA. mir-17, -155, and -191 are presented as positive control, and mir-15a as a negative control (grey boxes). 67% miRNAs tested are significantly up-regulated 30 min after induction, and pretreatment with BAY prevents this (*: $P<0.01$; $n=3$; unpaired two-tailed Student's *t*-test). Pre-miRNAs and miRNAs shown in red could not be detected.

Supplementary Figure S2

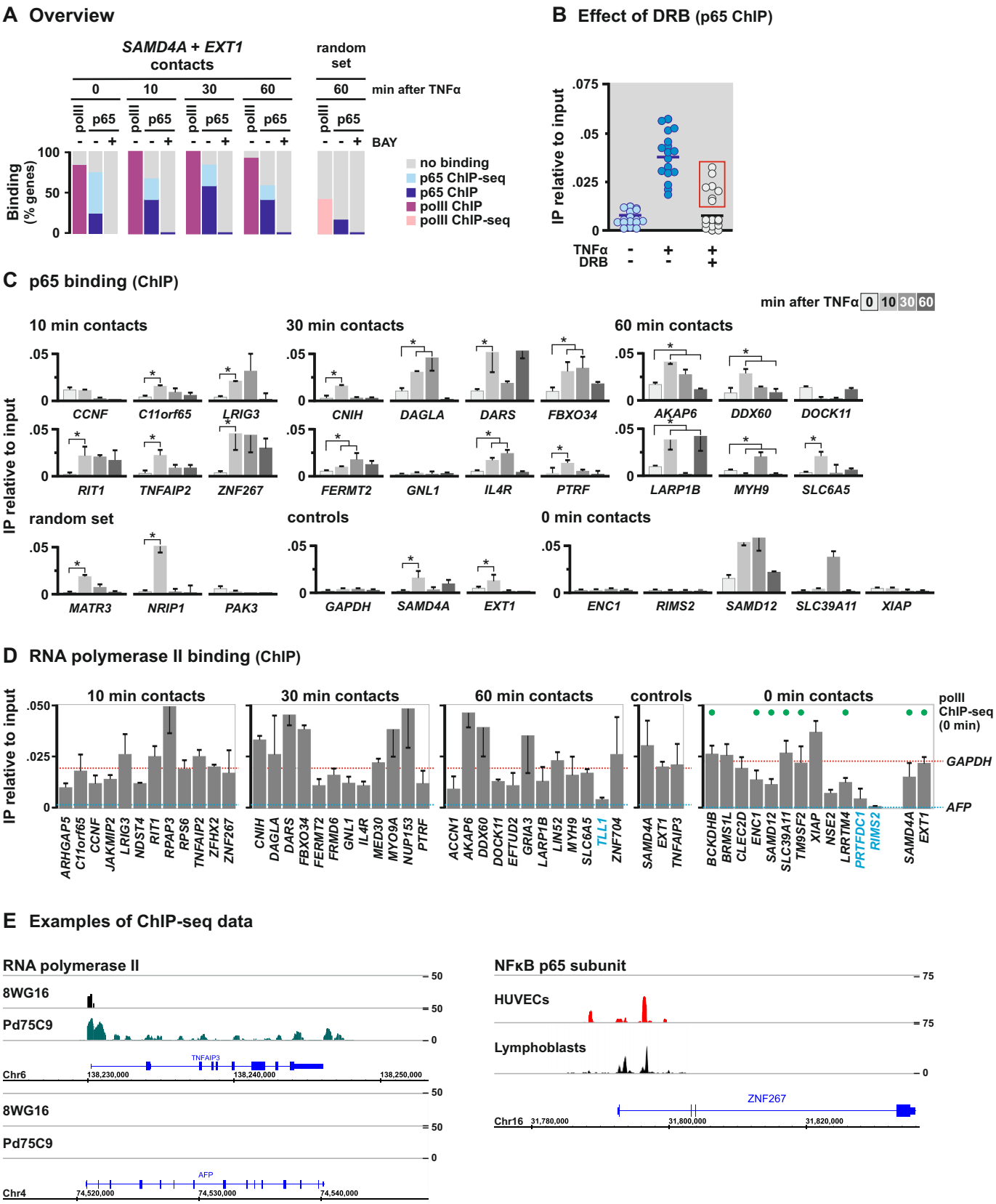

Supplementary Figure S2 ChIP shows that RNA polymerase II and the p65 subunit of NFκB bind to the promoters of most genes contacted by *SAMD4A* and *EXT1*. HUVECs were grown ± DRB for 1 h, treated with TNFα for up to 60 min, and binding of p65 and polymerase II monitored by ChIP at the relevant times (amount bound ± SD is expressed as a fraction of input; *n*=3). (**A**) Overview of results for sets of 12 randomly-selected genes contacted by *SAMD4A* and *EXT1*; a set of randomly-selected human genes provides a control. Contacts tend to bind the polymerase or p65 (compared to the random set), and BAY prevents this binding. Polymerase II binding to promoters (*i.e*., ±1 kbp of the TSS) was assessed by ChIP (ChIP-seq for the random set). Binding of p65 to genes possessing at least one binding site (5'-GGGRNNYCC-3') within 3 kbp upstream of the TSS was assessed by ChIP; binding to genes lacking such p65 binding motifs (as qPCR primers could not be designed) was assessed by ChIP-seq. (**B**) The transcriptional inhibitor, DRB, partially prevents p65 binding to the 17 promoters from the 10-, 30-, and 60-min sets in (A) and (C) that bound significantly more p65 after TNFα stimulation. Stimulation with TNFα increases binding to all promoters (line gives mean); DRB does not affect this increase for 7 out of the 17 genes tested (red box). (**C**) Details for the p65 ChIP presented in (A). *GAPDH* (plus *SAMD4A* and *EXT1*) provide additional negative (and positive) controls. Of the three genes in the random set that possessed at least 1 binding site, binding to only two increased significantly on stimulation. In contrast, binding to 5, 7, and 5 genes in the 10-, 30-, and 60-min sets, respectively, was significantly higher (*: $P<0.01$; unpaired two-tailed Student's *t*-test). (**D**) Details for the RNA polymerase II ChIP presented in (A). The *GAPDH* TATA box and the *AFP* 3' untranslated region are included as controls, as well as three responding promoters (*SAMD4A*, *EXT1*, *TNFAIP3*). Most promoters at each of the four times were associated with polymerase levels comparable to those of constitutively-expressed *GAPDH* (dotted red line). Only the *TLL1, PRTFDC1,* and *RIMS2* promoters (light blue) were associated with low levels seen with *AFP* (dotted blue line). (**E**) Typical genome browser views (IGB v. 6.4) of genes showing RNA polymerase II and p65 binding determined by ChIP-seq. *Left*: Results obtained using two different antibodies against RNA polymerase II (commercially-available 8WG16, and Pd75C9); a transcribed (*TNFAIP3*) and non-transcribed gene (*AFP*) which were tested in (D) are shown. *Right*: Results obtained using different antibodies targeting p65 using HUVECs or lymphoblasts (data for the latter from Kasowski *et al,* 2010); patterns are similar.

Supplementary Figure S3

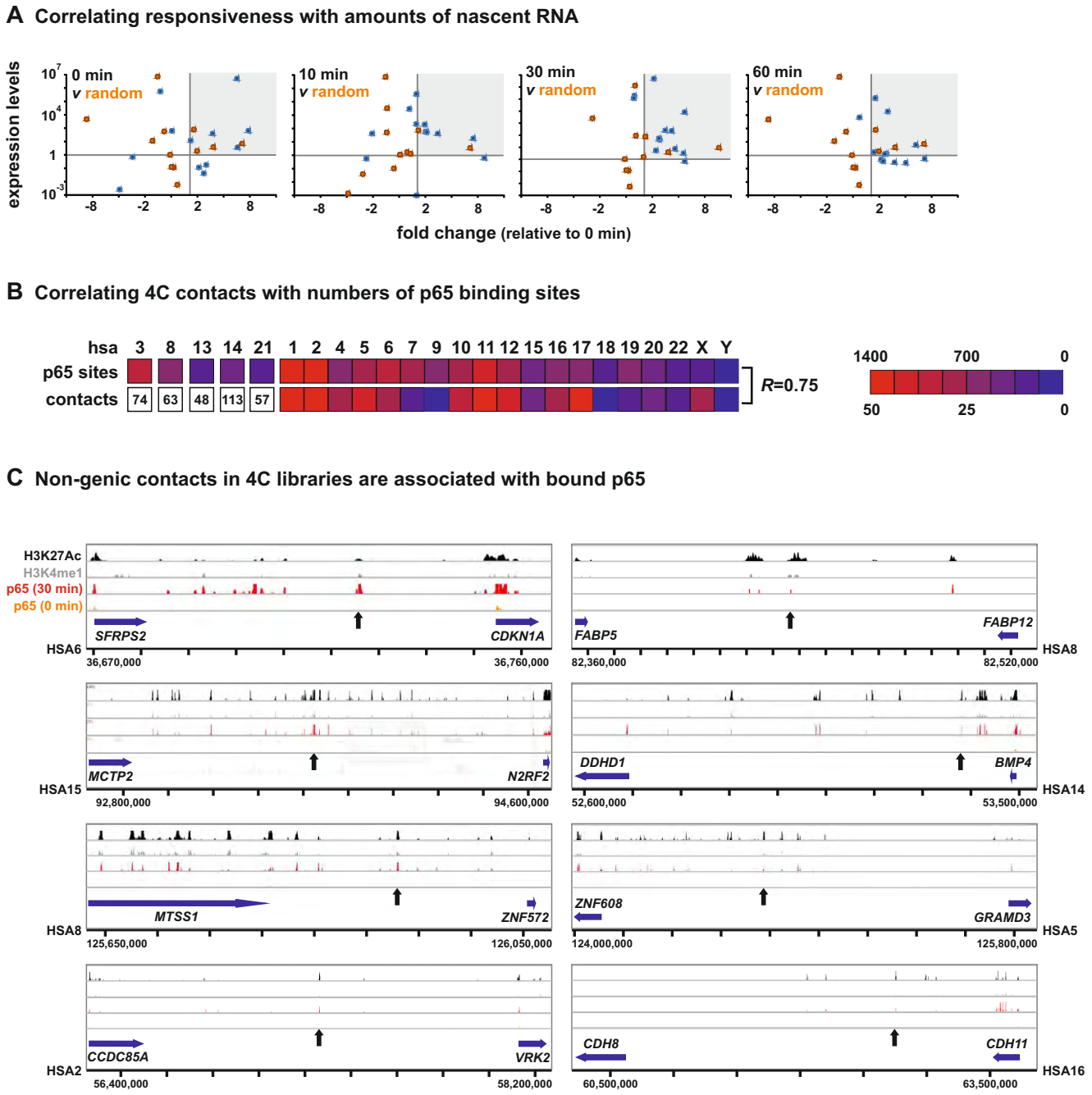

Supplementary Figure S3 Characteristics of contacts seen by 4C. Data is derived from 4C libraries prepared without BAY between 0-60 min after stimulation with TNFα and analyzed by conventional sequencing. (**A**) Correlation between TNFα responsiveness and the expression level of a gene. The four sets of 12 genes contacted by *SAMD4A* or *EXT1* and seen in 4C libraries 0, 10, 30, and 60 min after stimulation—plus the random control set—were analyzed (these sets were also analyzed in **Supplementary Figure S2A**). Fold change is the nascent RNA level at the time indicated relative to the 0-min level; expression level is the amount of nascent RNA normalized relative to the level of mature *RNU6* RNA. The horizontal grey line indicates the level given by *GAPDH*, and the vertical grey line marks 1.5-fold up-regulation. Many contacted genes (blue circles), but few in the random set (brown circles), are up-regulated more than 1.5-fold (and so lie in the two quadrants on the right); this confirms that contacted genes tend to be up-regulated. Of the minority of contacted genes that are not up-regulated, many tend to be transcribed more than *GAPDH* (and so lie in the top left quadrant). (**B**) The numbers of contacts made by *SAMD4A*, *EXT1*, *MIR17*, *MIR155*, and *MIR191* with different chromosomes (assessed using 4C) is compared with the number of p65 binding sites on each chromosome (determined using published ChIP-seq data; Kasowski *et al,* 2010). *Open boxes*: numbers of intra-chromosomal contacts made by each reference gene (*SAMD4A*, *EXT1*, *MIR17HG*, *MIR155HG*, and *MIR191* reside on chromosomes 14, 8, 13, 21, and 3, respectively) which were not included in the analysis. Pearson's correlation coefficient (*R*) for the two sets was 0.75; correlation coefficients for contact number and chromosomal length or site density/Mbp were significantly lower (*i.e.*, *R*=0.58 and 0.33, respectively). No contacts map to the Y chromosome, which is not present in (female) HUVECs. (**C**) Browser views (IGB v. 6.4) of eight of the 10 most-frequently seen non-genic contacts (the other two lacked any bound p65 and are not shown) seen in the 4C libraries. Vertical arrows indicate contact points; y-axis for each track in reads per million (from 0 to 50). In most cases, the contact point exhibits a peak in two "active" chromatin marks (*i.e.*, H3K27Ac and H3K4me1), as well as increased binding of p65 30 min after stimulation.

Supplementary Figure S4

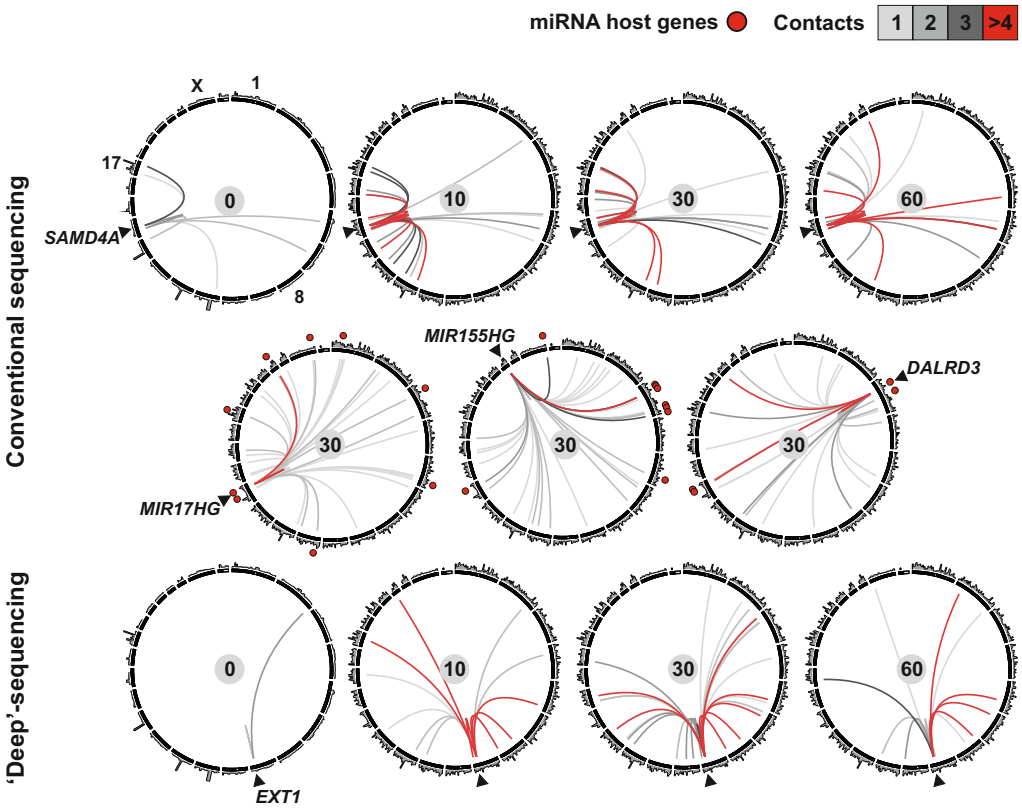

Supplementary Figure S4 Contacts evolve over time and contacting regions are rich in bound p65. Circos software (Krzywinski *et al,* 2009) was used to depict *SAMD4A, EXT1,* and miRNA contacts detected by 4C coupled to conventional or "deep"-sequencing. Chromosome ideograms are drawn to scale and presented clockwise from 1 to Y; positions of chromosomes 1, 8, X, and 17 are indicated, and no contacts are with the Y chromosome—which is not present in (female) HUVECs. Contacts are color-coded according to their frequency of occurrence (from light grey for singletons to red for >4 contacts). p65 ChIP-seq data are shown on the outer track (peak height reflects amount bound). *Arrowheads*: positions of reference genes. *Red* circles: gene hosting a micro-RNA. For simplicity, non-genic hits seen by 4C coupled to "deep"-sequencing are omitted. Results show that many new contacts appear after 10 min, and then contacts evolve thereafter. Note that reference genes contact other chromosomes more often than their own (*e.g*., ~60 of *SAMD4A* and ~84% of *EXT1* contacts are inter-chromosomal); globin genes frequently make such inter-chromosomal contacts (Brown *et al*, 2008; Schoenfelder *et al,* 2010). 47% *SAMD4A* contacts and 41% *EXT1* contacts are with chromosomes not contacted by the other—a percentage significantly higher than that expected by chance ($P < 10^{-100}$, calculated using the binomial distribution assuming chromosomes contact each other with equal probability); this is consistent with the respective territories lying in different parts of the nucleus. This differential location was confirmed by analyzing images like those in **Figure 4A**; 71% foci containing nascent RNA encoded by *SAMD4A*, compared to 43% *EXT1* foci, lay in the peripheral half of the nuclear area.

Supplementary Figure S5

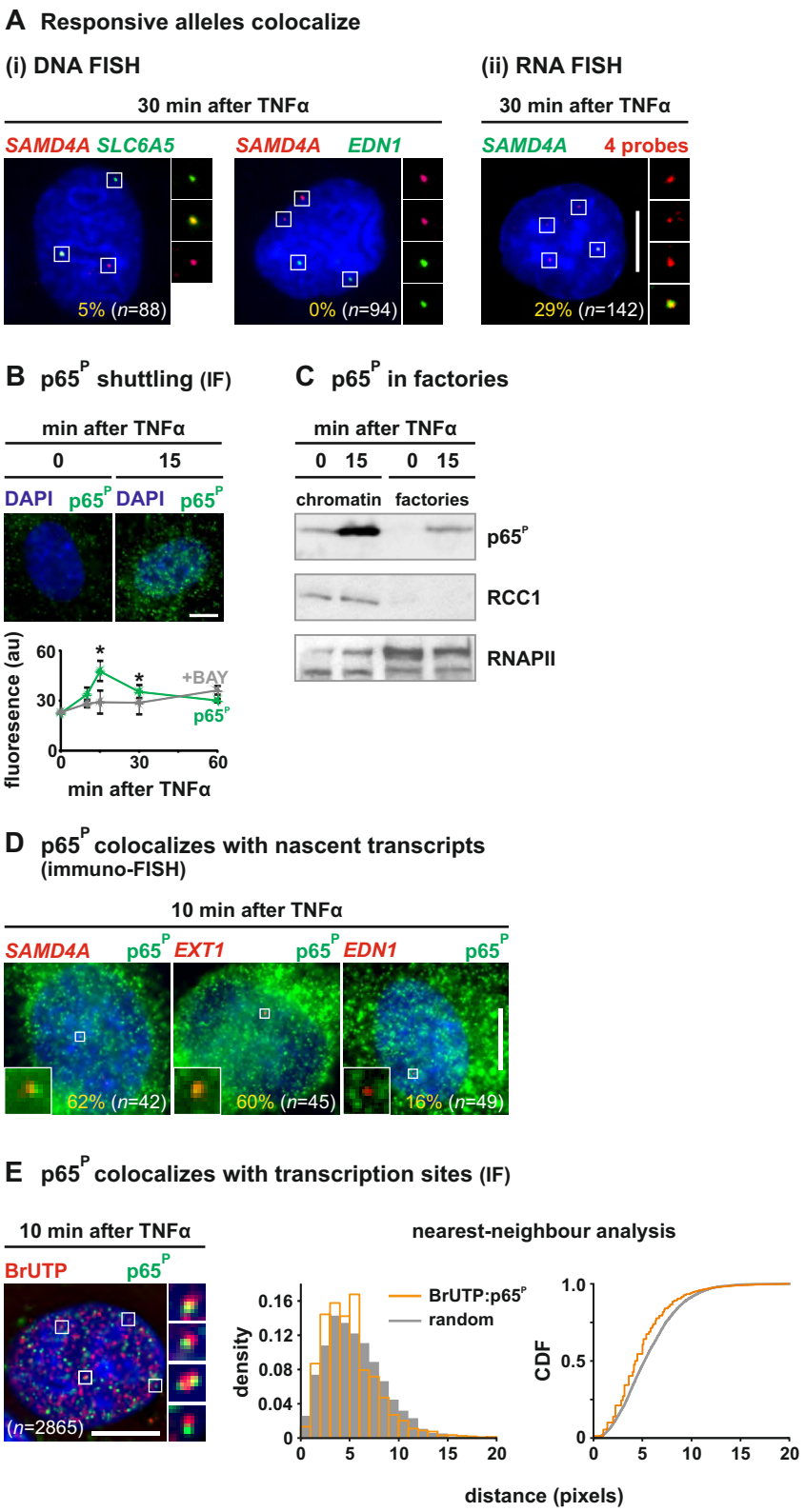

Supplementary Figure S5 *SAMD4A* and *EXT1* alleles/transcripts colocalize in NFκB-factories. HUVECs were stimulated using TNFα for 0-60 min in the presence or absence of the BAY inhibitor. *Bars*: 5 μm. (**A**) Responsive alleles colocalize 30 min after stimulation. (**i**) DNA FISH was performed using probes targeting *SAMD4A* (on HSA 14), *SLC6A5* (on 11), and *EDN1* (on 6). 5% nuclei screened (*n*=88) had at least one *SAMD4A* allele colocalizing with a *SLC6A5* allele (*left*); these two genes were shown to contact each other by 4C (**Supplementary Table S1**), and their nascent transcripts also colocalize (RNA FISH showed ~7% active alleles colocalized; Papantonis *et al*, 2010). A control targeting *SAMD4A* and constitutively-active *EDN1* (*right*) yielded no overlapping foci (*n*=94); this difference is statistically significant (*P*=0.0249; two-tailed Fisher's exact test). (ii) Nascent RNA FISH was performed as in Figure 4, using probes targeting *SAMD4A* (green) and a set of 4 multiplexed ones (red) on chromosomes 4, 5, 16, and 22; 29% (*n*=142) of green foci overlapped at least one red focus, significantly more than the 2% yielded by the control in Figure 4 (*P*<0.0001; two-tailed Fisher's exact test). (**B**) Phospho-p65 ($p65^P$; phosphorylated at Ser 536) shuttling. *Left*: the nucleus (DAPI-stained) contains more $p65^P$ 15 min after induction. *Right*: the intensity of nuclear fluorescence (arbitrary units, au) is significantly higher after 15 and 30 min, compared to 0 min or in BAY-treated cells (*: *P*<0.01; *n* = 20; unpaired two-tailed Student's *t*-test). (**C**) $p65^P$ becomes enriched in purified factories after stimulation. Nuclei were isolated from HUVECs, chromatin detached with DNase I, and spun to leave "chromatin" in the supernatant. The pellet was resuspended, treated with caspases, and spun; this supernatant contains large fragments of "factories" released from the substructure. $p65^P$, RNA polymerase II, and RCC1 (used as a negative control, as it is an abundant nuclear protein not present in factories; Melnik *et al,* 2011) in "chromatin" or "factories" were then detected by immuno-blotting. RNA polymerase II serves as a loading control. $p65^P$ becomes enriched in "factories" after 15 min, but not RCC1 is detected within factories at either time. (**D**) Nascent *SAMD4A* and *EXT1* transcripts colocalize with $p65^P$ after induction. Fixed cells were hybridized with intronic probes targeting *SAMD4A* or *EXT1* (or *EDN1*, a constitutively-expressed gene used as a control), and $p65^P$ immunolabeled. A single red focus in each nucleus marks nascent RNA copied from one allele; the insets show nascent *SAMD4A* and *EXT1* transcripts colocalize with $p65^P$ foci (green). 62% *SAMD4A* foci (*n*=42) and 60% *EXT1* foci (*n*=45) colocalize with $p65^P$ foci, significantly more (*P*=0.004 and 0.003, respectively; two-tailed Fisher's exact test) than the 16% found with *EDN1* foci (*n*=49). (**E**) Sites of active transcription colocalize with $p65^P$ after induction. HUVECs were stimulated for 10 min, permeabilized, and engaged polymerases allowed to "run on" by few nucleotides in BrUTP; nascent BrRNA and $p65^P$ were then visualized by immunolabeling. A typical wide-field image is shown (*left*; *insets* show magnified examples of overlapping red/green foci). Many red foci lie near green foci to give yellow in the merge. To assess whether the degree of colocalization was significant, foci were

selected automatically using a computer algorithm, peak intensities within the selected foci localized with 22-nm precision, and the distance from the peak of each red (or green) focus to its closest green (or red) focus determined (see **Supplementary methods**). A total of 2865 foci were analyzed. As a control, 8243 randomly-distributed foci with the same density were computer-generated. Plots (*right*) of probability density (density) and cumulative density function (CDF) versus distance to the nearest neighbour in the other channel (in pixels; 1 pixel=90 nm) show that $p65^{P}$ and BrRNA foci are significantly closer together than random (P<0.001, Kolmogorov-Smirnov two-sample test; compare orange and grey bins/lines; in the plot on the right, error bars ± 99% confidence limit are contained within the grey line). Note that the experimental sample gives a lower density in the first bin, which is consistent with one antibody (length ~9 nm) blocking access of a second to a nearby antigen.

Supplementary Figure S6

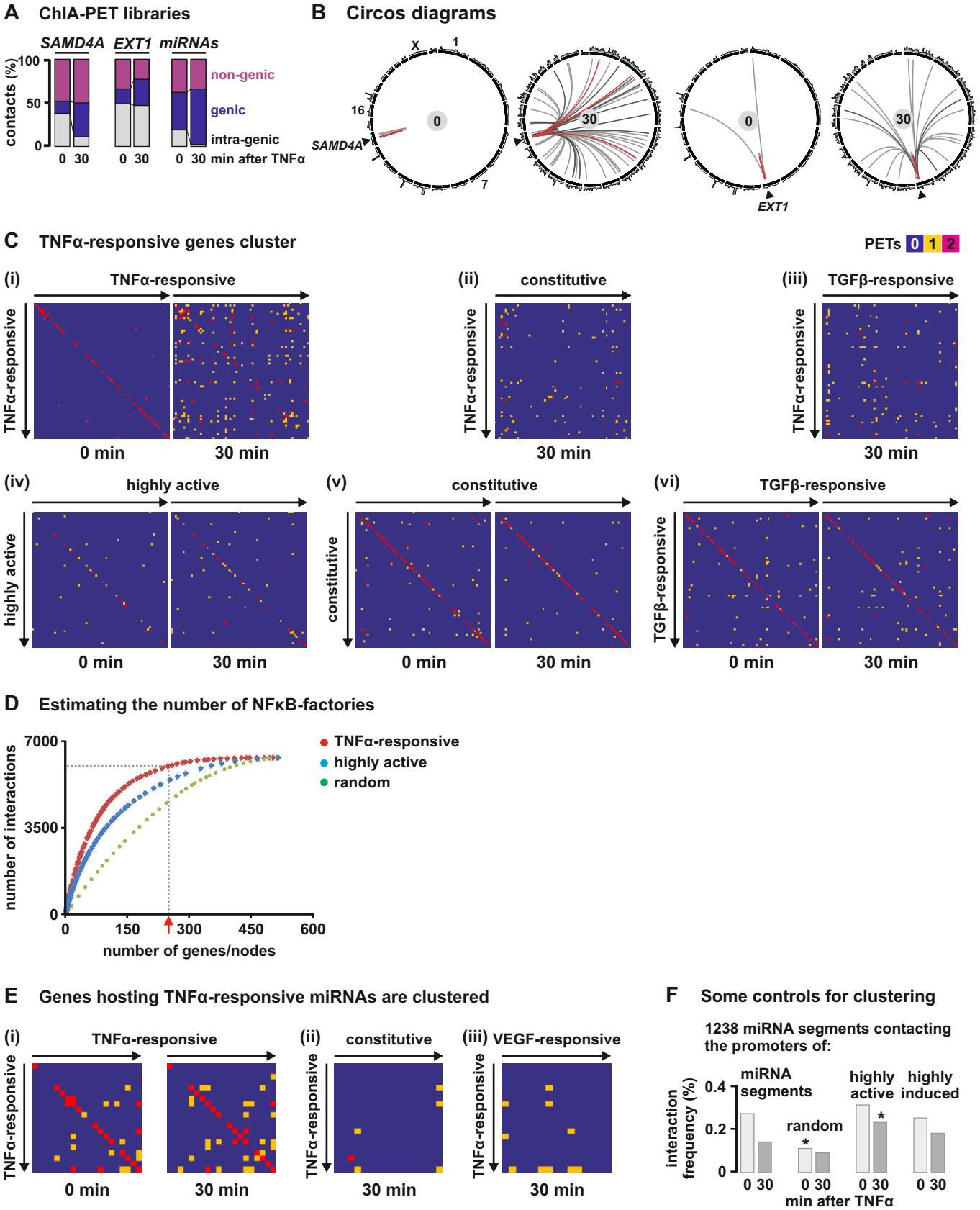

Supplementary Figure S6 ChIA-PET shows that TNFα-responsive genes, and genes encoding miRNAs, co-associate. HUVECs were grown in TNFα for 0 or 30 min, active forms of RNA polymerase II immuno-selected, ChIA-PET performed, and PETs (contacts) between selected genes analyzed. (**A**) Contacts made by *SAMD4A*, *EXT1*, and three miRNA genes (*MIR17*, *MIR155*, and *MIR191*; results pooled) classified as in **Figure 2A**. As for 4C, more genic contacts are detected after stimulation (see also **Supplementary Tables S5** and **S6**). (**B**) Contacts evolve over time. Circos software was used to depict contacts made by *SAMD4A* and *EXT1* (p65 ChIP-seq data is shown on the outer track). *Arrowheads*: positions of reference genes. For the sake of simplicity, non-genic hits are omitted. Results show that many new contacts appear after 30 min. (**C**) Stimulation induces TNFα-responsive genes to associate. Colored boxes within each matrix indicate no PET/contact between two genes (blue), 1 contact (yellow), or at least 2 contacts (red). Significance was assessed using Fisher's two-tailed exact test. (**i**) The 69 genes most up-regulated by TNFα versus the same 69 genes (reproduced from **Figure 5B** for comparison). Genes are ranked from high-to-low up-regulation (from left to right, and top to bottom), determined using microarray data obtained 0 and 30 min after stimulation (all up-regulated at least 1.9-fold). There are significantly more PETs/contacts between responsive genes at 30 min compared to 0 min ($P<0.0001$), and in the 30-min sample here compared to the 30-min samples in sub-panels (ii-vi), for which P values were <0.0001 in all cases. (**ii**) The 69 genes most up-regulated by TNFα versus a set of 69 randomly-chosen constitutively-active genes (of equivalent activity to the 69 genes up-regulated by TNFα). (**iii**) The 69 genes most up-regulated by TNFα versus the 69 genes most up-regulated by TGFβ (determined using microarrays, and ranked as above). (**iv**) The 69 most highly-active genes (but not up-regulated by TNFα) versus each other; there is no significant difference in the number of contacts between 0 and 30 min ($P=0.34$). (**v**) A set of 69 randomly-chosen constitutively-active genes (of equivalent activity to the 69 genes up-regulated by TNFα) versus each other. There was no significant difference in the number of contacts between 0 and 30 min ($P=0.06$). (**vi**) The 69 genes most up-regulated by TGFβ versus each other. There was no significant difference in the number of contacts between 0 and 30 min ($P=0.9$). (**D**) Estimating the number of "NFκB" factories. 496 genes, upregulated >3-fold, make 6,266 ChIA-PET contacts between them. If these 496 genes access essentially all "NFκB" factories in the cell, successively removing the gene making the fewest contacts from the set, and then the next fewest, and so on, should initially have little effect on the total number of interactions; this is the case. When too few up-regulated genes remain to saturate all "NFκB" factories, the number of interactions should begin to fall; ~250 genes recover ~95% interactions (dotted lines), and this provides us with an upper limit of the number of "NFκB" factories. Results for a random network (created by randomizing contacts in the observed network), and for the most-active, but non-responsive genes, are included for comparison.

(**E**) Genes hosting TNFα-responsive miRNAs cluster. The 20 genes encoding miRNAs were chosen because data from microarrays (Suárez *et al,* 2010) and qRT-PCR (**Supplementary Figure S1C**) showed they were up-regulated. Colored boxes within each matrix indicate 0 (blue), 1 (yellow), or at least 2 contacts (red) between two genes; genes are ranked (top to bottom, left to right) in order of increasing responsiveness. (**i**) The 20 responsive miRNA genes versus themselves at 0 and 30 min. Although the increase in the number of contacts is small (13 to 16, respectively; *P*=0.92) there is a noticeable rearrangement after stimulation. Most importantly, there are significantly more contacts in the 30-min sample here compared to those in sub-panels (ii) and (iii) (*P*=0.0021, and 0.0034, respectively; two-tailed Fisher's exact test). (**ii**) The 20 responsive miRNA genes versus a set of 20 constitutively-active miRNA genes (Suárez *et al,* 2010) 30 min post-stimulation. (**iii**) The 20 responsive miRNA genes versus a set of 20 VEGF-responsive miRNA genes (Suárez *et al,* 2008) 30 min post-stimulation. (**F**) Some additional controls for miRNA clustering. For the sake of completion, we also analyzed interactions between essentially all genes encoding miRNAs in the genome. We expect many miRNAs not to be expressed (Suárez *et al,* 2010), and thus would not expect members of this complete set of miRNA genes to interact more with themselves, compared to interactions with similarly-sized segments encoding expressed promoters; this proved to be the case. Essentially all segments of the genome encoding miRNAs were selected as follows. First, each of the 1,523 miRNAs in the database were mapped to the genome, each region extended +/- 5 kbp, and combined if they overlapped by >1 bp. Next, PETs/contacts were counted between the resulting 1238 "miRNA segments", these miRNA segments and an equal number of randomly-selected promoters (+/- 5 kbp), these miRNA segments and 886 or 890 promoters (+/- 5 kbp) at 0 or 30 min respectively that are the most highly-active but non-induced, and these miRNA segments and 879 highly-induced promoters (+/- 5 kbp) 30 min after stimulation. Finally, the interaction frequency (*i.e*., the number of PETs divided by the number of possible pairwise combinations expressed as a percentage) was calculated. No significant differences were seen, with the exceptions of randomly-selected promoters at 0 min, and highly-active promoters at 30 min (compared to miRNA segments at 0 and 30 min, respectively). *: *P*=<0.0001 (two-tailed Chi-squared test with Yates' correction). The higher interaction frequency seen after stimulation in panel (D,i) is consistent with the clustering of active miRNA genes—this is obscured by the large fraction of inactive miRNA genes in the sample used here.

Supplementary Figure S7

A Reproducibility in 4C libraries

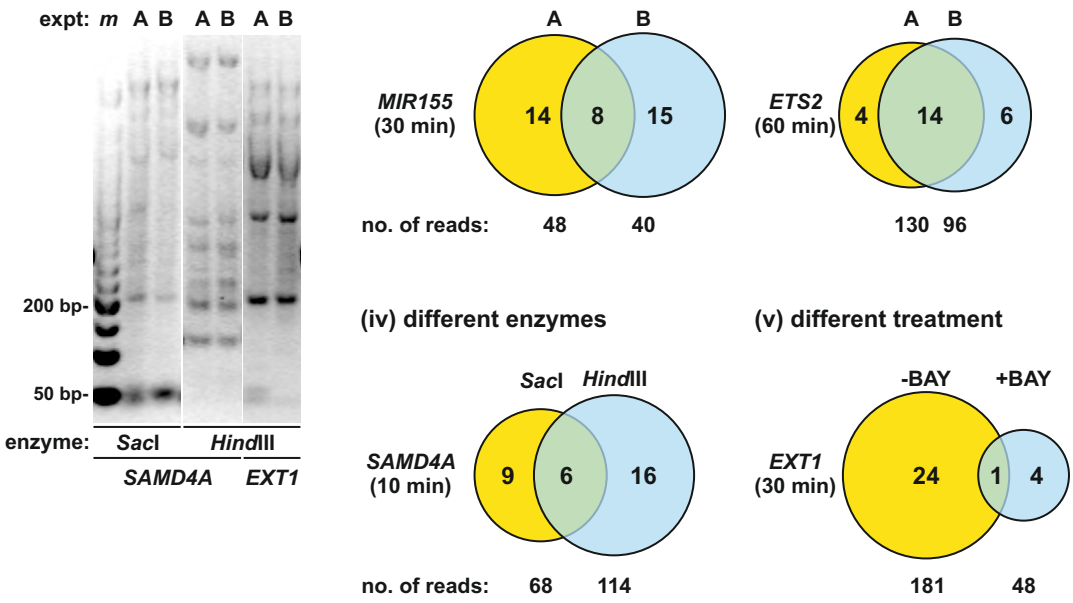

B Shared contacts between the different approaches

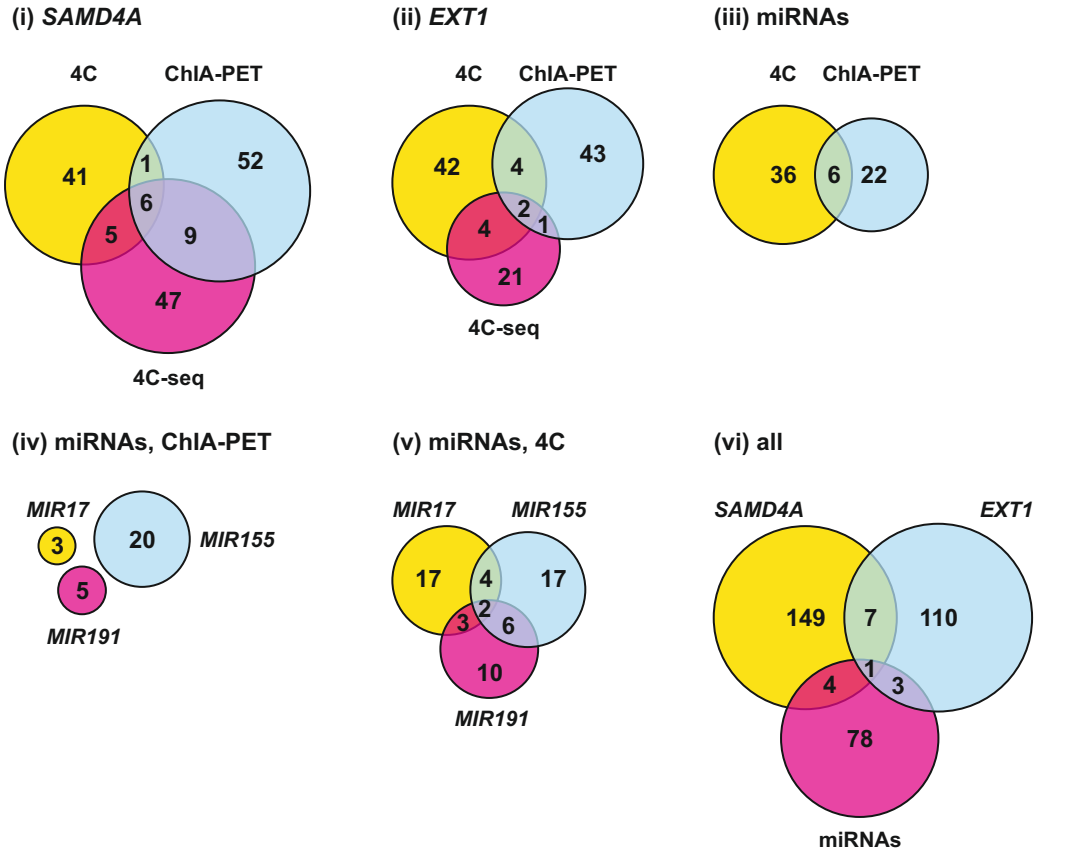

Supplementary Figure S7 Reproducibility between different libraries prepared and analyzed by 4C, 4C-seq, and ChIA-PET. Venn diagrams indicate the number of contacts shared between different libraries/approaches. (**A**) Comparison of both genic and non-genic contacts detected in different 4C libraries. (**i**) Representative examples of electrophoresis profiles after 4C and nested inverse PCR amplification between biological replicates (experiments A and B) using *SAMD4A* or *EXT1* as reference points, and *Sac*I or *Hind*III for cutting chromatin. *m*: marker DNA. (**ii**) Comparison between two libraries prepared using the same time after stimulation with TNFα (30 min), enzyme (*Hind*III), and reference gene (*MIR155*); ~36% contacts are shared, indicative of partial coverage. (**iii**) Comparison between two libraries prepared using the same time after stimulation with TGFβ (60 min), enzyme (*Hind*III), and reference gene (*ETS2*); as the number of 3C products screened is greater than in (ii), more contacts are shared (~74%). (**iv**) Comparison between two libraries prepared using the same time after stimulation with TNFα (10 min) and reference gene (*SAMD4A*), but different enzymes (*i.e*., *Hind*III and *Sac*I, yellow and blue, respectively); ~30% contacts in each are shared. (**v**) Comparison between two libraries prepared at the same time after stimulation (30 min) using the same reference point (*EXT1*), but with different treatments (*i.e*., addition or not of BAY); only 1 contact is shared. (**B**) Comparison of genic contacts detected using different 3C variants 0-60 min after TNFα stimulation. (**i**) *SAMD4A* contacts detected by 4C coupled to conventional sequencing ("4C"), 4C coupled to deep-sequencing ("4C-seq"), and ChIA-PET; ~13% 4C contacts are shared between all three approaches, ~22% between 4C and 4C-seq, and ~24% between 4C-seq and ChIA-PET. (**ii**) *EXT1* contacts detected by 4C coupled to conventional sequencing, 4C coupled to deep-sequencing, and ChIA-PET; ~7% 4C-seq contacts are shared between all three approaches. (**iii**) Contacts between genes hosting miRNAs detected by 4C and ChIA-PET; ~21% ChIA-PET contacts are shared. (**iv**) Contacts between genes hosting miRNAs detected using ChIA-PET; no contacts were shared, indicative of low coverage. (**v**) Contacts between genes hosting miRNAs detected using 4C; ~17% of *MIR191* contacts are now shared with both *MIR17* and *MIR155*. (**vi**) Comparison of pooled contacts (detected using all 3C variants) made by *SAMD4A*, *EXT1*, and three miRNA host genes; <1% contacts are shared between all three, indicative of distinct interactomes for each gene.

Supplementary Figure S8

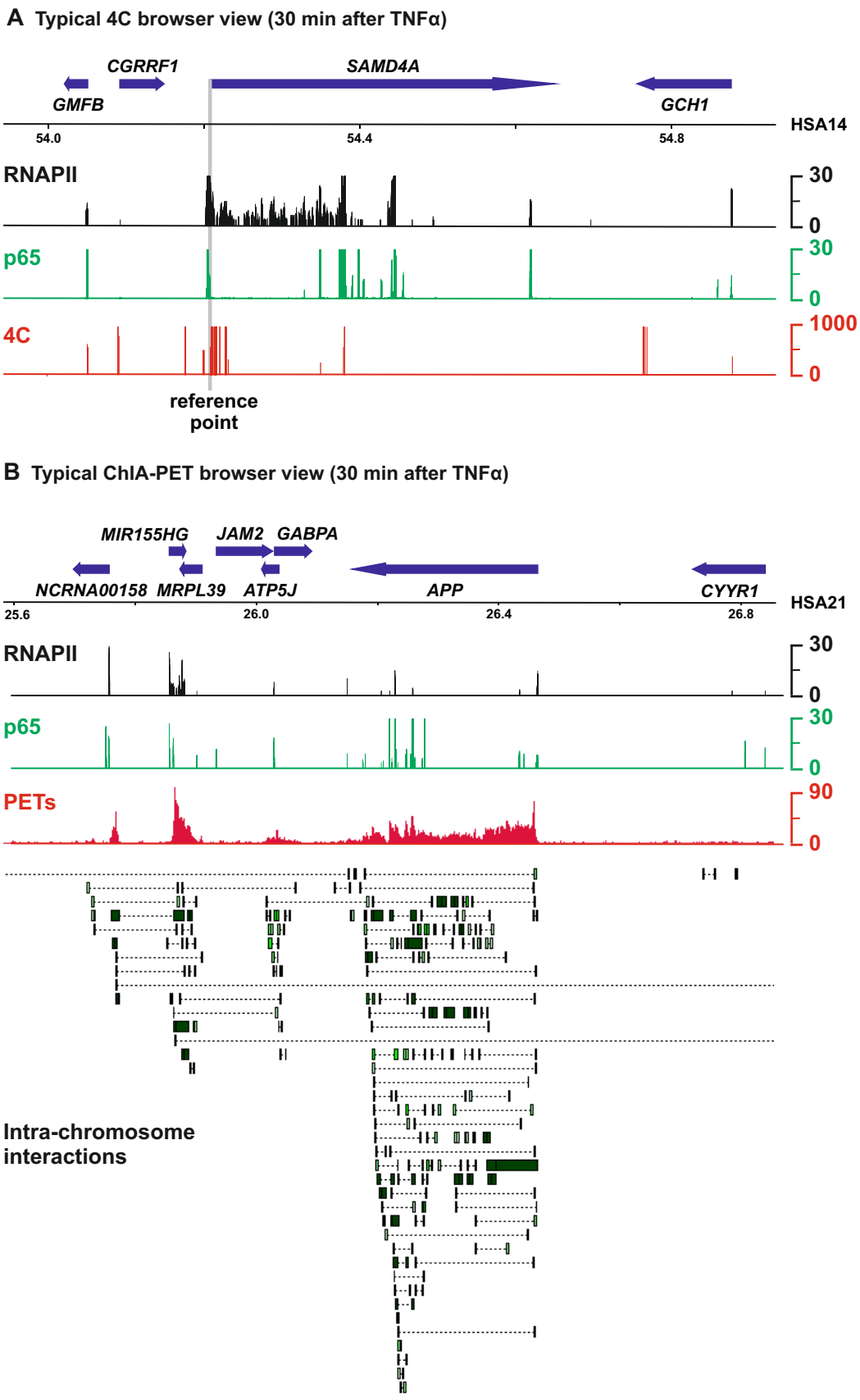

Supplementary Figure S8 Typical browser views of 4C-seq and ChIA-PET data obtained 30 min after stimulation. The number of reads per million for different genomic regions (*y*-axis) are shown for data from ChIP-seq (RNA polymerase II—*black*; p65—*green*), and 4C coupled to next-generation sequencing (*red*); the number of PETs (*y*-axis) is given for ChIA-PET data (*red*). (**A**) Region of ~1 Mbp around *SAMD4A*. *Grey line*: position of the TSS of *SAMD4A* used as the reference point for 4C. (**B**). Region of ~1 Mbp around *MIR155HG*. PETs (rectangles connected by dotted lines) in this part of the genome are shown at the bottom.

Legends to Supplementary Tables

Supplementary Table S1 Properties of genic contacts seen after conventional sequencing in 16 4C libraries prepared using *SAMD4A* and *EXT1* as reference points. Libraries were prepared using *Hind*III or *Sac*I 0-60 min after adding TNFα, and ~80 inserts in each sequenced. Gene name, chromosomal location, time(s) after stimulation when seen, the number of times seen (hits; the number of sequenced clones including identical ones), and TNFα responsiveness plus p65/RNA polymerase II binding (red and blue boxes indicate responsiveness/binding and non-responsiveness/non-binding, respectively, as in **Figure 2B**) are indicated. A random set of genes provides a control. *Grey highlight*: gene seen in at least two different libraries. *: gene randomly selected from those contacted at one time for detailed analysis (see **Supplementary Figures S1** and **S2**). *Orange highlights*: genes hosting miRNAs (*GCH1, PRKCA*, *STRN3*, and *MIR15A* encode mir-4308, -634, -624, and -15a, respectively). Over-representation of red boxes in the *SAMD4A* (43%; *n*=53) and *EXT1* (29%; *n*=52) columns (compared to random sample; *n*=75) indicates that significantly more contacted genes both respond to the cytokine and bind p65 and RNA polymerase II ($P<0.0001$ and 0.0011, respectively; two-tailed Fisher's exact test). Results obtained with each of the two enzymes were broadly similar.

Supplementary Table S2 Properties of genic contacts seen after "deep" sequencing 4C libraries prepared using the TSS of *EXT1* or *SAMD4A* as a reference. All genic contacts detected in libraries prepared using *Hind*III are listed, with chromosomal location, time(s) after stimulation when seen, the number of different sites contacted within the gene (hits; this definition differs from that in **Supplementary Table S1**), and TNFα responsiveness plus p65/RNA polymerase II binding (red and blue boxes indicate responsiveness/binding and non-responsiveness/non-binding, respectively, assessed as in **Figure 2B**). *Grey highlight*: gene also detected by conventional sequencing or ChIA-PET (**Supplementary Tables S1** and **S5**). *Orange boxes*: genes hosting miRNAs. Over-representation of red boxes (compared to the random sample in **Supplementary Table S1**) indicates that significantly more contacted genes are responsive and bind p65/RNA polymerase II. For example, 34% (*n*=50) *EXT1* and 27% *SAMD4A* (*n*=67) contacts are responsive and bind both p65 and the polymerase—significantly more than the 7% (*n*=75) in the random set ($P=0.0002$ and 0.0024, respectively; two-tailed Fisher's exact test).

Supplementary Table S3 Properties of genic contacts seen after conventional sequencing in 4C libraries prepared using genes encoding mir-17, -155, and -191 as reference points. Libraries were prepared using *Hind*III at 30 min after adding TNFα, and ~96 inserts in each sequenced. Gene name, miRNA encoded, chromosomal location, the number of times seen (hits; the number of sequenced

clones including identical ones), and TNFα responsiveness plus p65/RNA polymerase II binding (red and blue boxes indicate responsiveness or binding and non-responsiveness or nonbinding, respectively, assessed as in **Figure 2B**), are indicated. *Grey highlight*: gene hosting one or more miRNAs. Comparisons of the combination of the three sets (*n*=75) with the random sample (*n*=75) or the *SAMD4A* contacts (*n*=53) in **Supplementary Table S1** show significant enrichment in miRNA-hosting genes (*P*<0.0001 and 0.0012, respectively; two-tailed Fisher's exact test).

Supplementary Table S4 Micro-RNAs encoded by three reference genes (*MIR17HG*, *MIR155HG*, and *MIR191/DALRD3*) and their contacts target mRNAs down-regulated by TNFα. The lists depict the 100 genes most down-regulated by TNFα 1 and 4 h after stimulation (selected using microarray data, and listed in order of the most down-regulated to the least); 100 randomly-selected genes serve as a control. Gene name and ratios of expression (compared to 0 min levels) are given. Grey highlights indicate that the 3' UTR of the corresponding mRNA possesses one or more targets for the miRNAs encoded by the three reference host genes and their contacts. Contacted genes encoding miRNAs are listed in **Supplementary Figure S1C**, and the mRNA targets of these miRNAs were detected using the algorithm in the miRWalk database. The down-regulated genes (*n*=200) encode mRNAs with significantly more (*P*=0.0082; two-tailed Fisher's exact test) target sites for the miRNAs encoded by the contacted genes, when compared to the random set (*n*=100).

Supplementary Table S5 Properties of *SAMD4A* and *EXT1* genic contacts detected by ChIA-PET. ChIA-PET libraries were prepared 0 or 30 min after TNFα stimulation and genic contacts formed by *SAMD4A* and *EXT1* mined from the genome-wide interactome. Contacts are listed in rank order of number of PETs seen with gene name, number of PETs seen (only >2 PETs listed), chromosomal location, and TNFα responsiveness plus p65/RNA polymerase II binding (red and blue boxes indicate responsiveness/binding and non-responsiveness/non-binding, respectively, as in **Figure 2B**). *Grey highlight*: contacts also seen by 4C. As in the 4C libraries (**Figure 2A**), more contacts develop after 30 min. *Dots*: contacted genes that are pre-loaded with RNA polymerase at 0 min (from ChIP-seq data). Over-representation of red boxes (compared to the random sample in **Supplementary Table S1**) indicates that significantly more contacted genes are responsive and bind p65/RNA polymerase II. For example, 48.5% (*n*=50) *SAMD4A* and 35.7% (*n*=28) *EXT1* contacts are responsive and bind both p65 and the polymerase—significantly more than the 6.67% (*n*=75) in the random set (*P*<0.0001 and 0.0006, respectively; two-tailed Fisher's exact test).

Supplementary Table S6 Properties of genic contacts made by genes hosting mir-17, -155, and -191 (detected by ChIA-PET). ChIA-PET libraries were prepared 0 or 30 min after TNFα stimulation and contacts formed by *MIR17HG, MIR155HG* and *DALRD3* (which hosts miR-191) mined from the complete genome-wide interactome. Contacts are listed in rank order of number of PETs seen with gene name, number of PETs seen (all PETs detected are listed), chromosomal location, name of hosted miRNAs, and TNFα responsiveness plus p65/RNA polymerase II binding (red and blue boxes indicate responsiveness or binding and non-responsiveness or non-binding, respectively, assessed as in **Figure 2B**). *Grey highlight*: contacts that involve miRNA-hosting genes; genes encoding non-coding RNAs (NCRNA or LOC) are also shown. Comparison of each of the three sets (n=28, 189, and 51, respectively) with the random sample (n=75) in **Supplementary Table S1** shows significant enrichment in miRNA-hosting genes (P=0.0054, 0.0022, and 0.0174, respectively; two-tailed Fisher's exact test).

Supplementary Table S7 Some genic contacts seen in 4C libraries (prepared using *SAMD4A* and *EXT1* as reference points) are TGFβ-responsive. Gene name, chromosomal location, time(s) after stimulation when seen, the number of times seen (hits; the number of sequenced clones including identical ones), and TNFα responsiveness plus p65/RNA polymerase II binding (red and blue boxes indicate responsiveness/binding and non-responsiveness/non-binding, respectively, as in **Figure 2B**) are indicated. Some contacted genes (28% and 40% for *SAMD4A* and *EXT1*, respectively) are responsive to both TNFα and TGFβ, revealing some overlap between the two pathways. However, responsiveness to TNFα and TGFβ appears uncorrelated (R=0.19 and 0.16 for *SAMD4A* and *EXT1*, respectively), consistent with contacts made by these two reference genes being specific for the TNFα cascade.

Supplementary Table S1. Properties of genic contacts seen after conventional sequencing in 4C libraries prepared using *SAMD4A* and *EXT1* as reference points.

***SAMD4A* contacts**

gene	chr	time	hits	array	ChIP-seq p65	ChIP-seq pol II
**FBXO34*	14	30,60	8			
**TNFAIP2*	14	10,30,60	8			
C10orf12	10	30	7			
**FERMT2*	14	30,60	7			
**IL4R*	16	30,60	7			
**LARP1B*	4	60	7			
AP4S1	14	60	6			
**ARHGAP5*	14	10	6			
**CCNF*	16	10	6			
**FRMD6*	14	30	6			
GCH1	14	10,30,60	6			
PRKCA	17	30	6			
ATP8A2	13	10	5			
**MYH9*	22	60	5			
PRKD1	14	10	5			
**SLC6A5*	11	10,30,60	5			
**AKAP6*	14	60	4			
**C11orf65*	11	10	4			
**CNIH*	14	30	4			
**GNL1*	6	30	4			
KRT6B	12	10	4			
**PTRF*	17	10	4			
**SLC39A11*	17	0,10,30	4			
ZNF608	5	60	4			
**ACCN1*	17	60	3			
C14orf43	14	30	3			
C14orf50	14	30	3			
C14orf70	14	30	3			
CGRRF1	14	30	3			
CITED2	6	60	3			
DDHD1	14	60	3			
KLF12	13	10	3			
**LIN52*	14	60	3			
LRRIQ1	12	60	3			
SNX24	5	10,30	3			
TMCC3	12	10	3			
**BRMS1L*	14	0,10	3			
**ZNF267*	16	10,30	3			
ABCA3	16	10	2			
ARHGEF17	11	10	2			
CALR3	19	60	2			
CDKN3	14	30	2			
**EFTUD2*	17	60	2			
FAM179B	14	30	2			
PSMC1	14	10	2			
SPAG16	2	10	2			
STRN3	14	60	2			
**TM9SF2*	13	0	2			
**BCKDHB*	6	0	2			
**ENC1*	5	0	2			
**ZFHX2*	14	10	2			
VEZF1	17	30	2			
**PRTFDC1*	10	0	1			

EXT1 contacts

gene	chr	time	hits	array	ChIP-seq p65	ChIP-seq pol II
**JAKMIP2*	5	10,30,60	9			
**DAGLA*	11	0,10,30	8			
FGGY	1	30	8			
**SAMD12*	8	0-60	8			
C2orf55	2	60	7			
**DARS*	2	30	7			
**DOCK11*	X	60	7			
KIF21A	12	30	7			
**NUP153*	6	30	7			
SLC30A8	8	10,30,60	7			
BAGE	21	60	6			
CCDC54	3	10,30,60	6			
CHRDL1	X	60	6			
CLEC2D	12	10,30,60	6			
**DDX60*	4	60	6			
FLJ21511	4	60	6			
**GRIA3*	X	30,60	6			
ABCA9	17	10	5			
DLG2	11	30	5			
KIF1B	1	10	5			
**MYO9A*	15	30	5			
CAST	5	10	4			
LCOR	10	30	4			
RNF43	17	10	4			
**RPAP3*	12	10,30	4			
TGFA	2	30	4			
YT521	4	60	4			
**ZNF704*	8	60	4			
**LRIG3*	12	10	3			
**LRRTM4*	2	0	3			
**MED30*	8	30	3			
OAS2	12	30	3			
RGS22	8	30	3			
TPTE	21	10	3			
TTC21B	10	30	3			
C10orf76	10	60	2			
CHST11	12	30	2			
DCTN6	8	30	2			
KCNAB1	3	30	2			
PIGW	17	30	2			
RBPMS	8	30	2			
RELN	7	30	2			
**RIMS2*	8	0	2			
**RIT1*	1	10	2			
**TLL1*	4	60	2			
RNLS	10	10	2			
**RPS6KA2*	6	10	2			
MATR3	5	60	2			
**NDST4*	4	10	2			
**XIAP*	X	0	2			
WSB1	17	0,10	2			
**NSE2*	8	0	1			

random set

gene	chr	array	ChIP-seq p65	ChIP-seq pol II
ABCC9	12			
ADARB1	21			
ANKS1B	12			
ANO1	11			
BAG1	9			
BMP2K	4			
BRD7	16			
C20orf57	20			
C2orf51	2			
C4A	6			
CARD18	11			
CATSPER3	5			
CBL	11			
CBX3	7			
**CCDC42*	17			
CIDEC	3			
CLK4	5			
CPSF2	14			
DDX24	14			
DHX9	1			
DLL4	15			
ELF5	11			
ESR1	6			
EXOSC7	3			
FAM179B	14			
FAM73A	1			
FGF18	5			
**GAPDH*	12			
GIMAP1	7			
GLT8D4	3			
GPR112	X			
HIST1H3I	6			
HNRPA3	2			
IFT81	12			
**IL1RAPL2*	X			
ITIH5	10			
KRT37	17			
LATS2	13			
LEP	7			
LHFPL5	6			
**LRRC7*	1			
LZTS2	10			
MAN1A2	1			
**MATR3*	5			
METT10D	17			
MFAP5	12			
**MIR15A*	13			
MRPL39	21			
NCLN	19			
**NRIP1*	21			
NUDCD1	8			
OMD	9			
**PAK3*	X			
PARP15	3			
PCSK6	15			
PHF14	7			
POLR2B	4			
**RCOR1*	14			
**RGMA*	15			
RFX2	19			
RHOU	1			
SFRS2B	11			
SGEF	3			
SLC16A3	17			
SSFA2	2			
**SSTR1*	14			
STYK1	12			
TANC2	17			
TIMP2	17			
TMEM203	9			
**TOX*	8			
TRIML2	4			
WWOX	16			
ZNF229	19			
ZNF460	19			

Supplementary Table S2. Properties of genic contacts seen after "deep" sequencing 4C libraries prepared using the TSS of *EXT1* or *SAMD4A* as a reference.

***EXT1* contacts detected by circular 3C-seq**

gene name	chr	time	hits	array	ChIP-seq p65	ChIP-seq polII
BAGE	21	10,60	20			
SAMD4A	14	30	17			
ZNF608	5	30,60	16			
SYN2	3	30	14			
CAMK2B	7	10,30,60	13			
MLL3	7	10	13			
ASAP2	2	60	10			
TRAPPC9	8	10	10			
GLO1	6	30	9			
SKAP1	17	10	8			
SCYL2	12	30	7			
ZNF322A	6	60	6			
SLU7	5	10	5			
PAXIP1	7	30	5			
SLC30A8	8	30	4			
RYR3	15	60	4			
FAM135B	8	30	3			
TEK	9	30	3			
C9ORF135	9	30	3			
RAPGEF1	9	60	3			
C11ORF65	11	30	3			
PRMT8	12	30	3			
DCTN5	16	30	3			
SNED1	2	0	3			
SATB2	2	30	2			
RAPH1	2	10	2			
KIF15	3	30	2			
FLJ21511	4	10	2			
TXNDC5	6	30	2			
ZFPM2	8	60	2			
SAMD12	8	60	2			
C9ORF98	9	30	2			
RBM20	10	10	2			
HTRA1	10	60	2			
DCDC1	11	10	2			
METTL3	14	30	2			
TOX4	14	30	2			
TMPRSS11	4	30	1			
FAM5B	1	30	1			
SUMF1	3	30	1			
SCN5A	3	30	1			
DPYSL3	5	30	1			
GUCY2C	12	30	1			
ANKS1B	12	10	1			
CA12	15	10	1			
MGC33894	17	30	1			
MIR663B	2	30	1			
CCDC146	7	10	1			
ALPPL2	2	10	1			
ARHGAP6	X	30	1			

***SAMD4A* contacts detected by circular 3C-seq**

gene name	chr	time	hits	array	ChIP-seq p65	ChIP-seq polII
CGRRF1	14	30	80			
GCH1	14	30	30			
GMFB	14	30	23			
WDHD1	14	30	20			
CNIH	14	30	11			
CDKN3	14	30	8			
TNFAIP2	14	30	6			
FERMT2	14	30	5			
SOCS4	14	30	5			
DPF3	14	30	4			
FRMD6	14	30	4			
MAPK1IP1L	14	30	4			
RAD51L1	14	30	4			
DLGAP5	14	30	3			
TTC7B	14	30	3			
C14orf159	14	30	2			
C14orf179	14	30	2			
CCDC88C	14	30	2			
CCNK	14	30	2			
DAAM1	14	30	2			
ERO1L	14	30	2			
FBXO34	14	30	2			
FLRT2	14	30	2			
HNRNPC	14	30	2			
KTN1	14	30	2			
LGALS3	14	30	2			
LIN52	14	30	2			
MIR541	14	30	2			
NID2	14	30	2			
PGF	14	30	2			
PPP1R13B	14	30	2			
PPP2R5E	14	30	2			
PSMA6	14	30	2			
GARNL1	14	30	2			
RHOJ	14	30	2			
RIN3	14	30	2			
RPS6KA5	14	30	2			
SOS2	14	30	2			
SYNE2	14	30	2			
TRIM9	14	30	2			
C14orf133	14	30	2			
ZFYVE26	14	30	2			
APP	21	30	2			
ATP5I	4	30	2			
CMTM7	3	30	2			
EIF4A3	17	30	2			
EPHA4	2	30	2			
FLNB	3	30	2			
GNAQ	9	30	2			
GPC3	X	30	2			
IQGAP1	15	30	2			
KLHL1	13	30	2			
KLHL3	5	30	2			
KSR2	12	30	2			
MED31	17	30	2			
MYH10	17	30	2			
MYH9	22	30	2			
OSBPL9	1	30	2			
PRKG1	10	30	2			
QKI	6	30	2			
RGNEF	5	30	2			
SLC6A5	11	30	2			
SLIT3	5	30	2			
SPOCK1	5	30	2			
FZD4	11	30	2			
TRIO	5	30	2			
UTRN	6	30	2			

Supplementary Table S3. Properties of genic contacts seen after conventional sequencing in 4C libraries prepared using genes encoding miR-17, -155, and -191 as reference points.

mir-17 contacts

gene name	miRNA	chr	hits	array	ChIP-seq p65	ChIP-seq polII
GPC5		13	7			
MIR155HG	-155	21	6			
SKAP1	-1203	17	2			
DALRD3	-191	3	2			
FARP1	-3170	13	2			
BTG3		21	2			
FGF13	-504	X	2			
FAM81A		15	2			
INPP5A		10	2			
NCRNA00264		10	2			
HADHB		2	2			
EVI1		3	2			
BRF1		14	1			
CCT8L2		22	1			
PCDH9		13	1			
UBE3A		15	1			
MBD5		2	1			
PRKD1		14	1			
MIR3169	-3169	13	1			
MYO3A		10	1			
FLJ21511		4	1			
FBXO46		19	1			
NRD1	-761	1	1			
PERC	-378	5	1			
RANBP3		19	1			
SBF2		11	1			

mir-155 contacts

gene name	miRNA	chr	hits	array	ChIP-seq p65	ChIP-seq polII
NDUFAF3	-425	3	5			
DALRD3	-191	3	4			
GABRA3	-105/-767	X	4			
LPP	-28	3	4			
MIR17HG	-17	13	3			
NCRNA00158		21	2			
STXBP5		6	2			
FSTL4	-1289	5	2			
INPP5A		10	2			
MIR1263	-1263	3	2			
CELF2		10	2			
EVI1		3	2			
HTR7		10	2			
LHFP		13	2			
TMEM204		16	2			
BTBD9		6	2			
FAP		2	1			
HERC2		15	1			
SGEF		3	1			
EXOSC7		3	1			
CBL		11	1			
MRPL39		21	1			
CR1L		1	1			
ATRIP		3	1			
MIR720	-720	3	1			
MIR4272	-4272	3	1			
NCAM2		21	1			
HADHB		2	1			
SBF2		11	1			

mir-191 contacts

gene name	miRNA	chr	hits	array	ChIP-seq p65	ChIP-seq polII
MACROD2		20	6			
EXOSC7		3	6			
MIR17HG	-17	13	5			
STARD3NL		7	3			
FMNL1		17	3			
NDUFAF3	-425	3	3			
CBL		11	3			
FARP1	-3170	13	2			
BTG3		21	2			
CNTN5		11	2			
COG6	-711	3	2			
TBC1D19		4	2			
QRICH1		3	2			
SGEF		3	2			
EVI1		3	1			
DNAH12		3	1			
INPP5A		10	1			
FAM98A		2	1			
LHFP		13	1			
ARIH2		3	1			
PFKFB4		3	1			

Supplementary Table S4. miRNAs encoded by three reference genes (*MIR17HG* , *MIR155HG* , *MIR191*) and their contacts target mRNAs down-regulated by TNFα.

Most down-regulated genes at: 1h after TNFα			4h after TNFα			random set		
gene name	ratio	miRNA	gene name	ratio	miRNA	gene name	ratio	miRNA
COL1A2	0.052	-29a/-29b	*TBX1*	0.021	-17	*LRRC7*	0.118	-
ZNF710	0.103	-	*SMAD7*	0.026	-17/-720/-1289	*NFX1*	0.125	-
ALPK1	0.106	-	*STAT4*	0.045	-	*SSTR1*	0.162	-
GJB3	0.112	-	*CISH*	0.048	-29a/-155	*STYK1*	0.179	-1265
PPP1R3C	0.112	-1203	*KIAA0644*	0.062	-	*KLF16*	0.200	-
APC	0.119	-17/-155	*SORBS1*	0.063	-378/-3169	*PAK3*	0.247	-17/-28-5p/-155
DYRK1A	0.132	-28-5p/-3169/-4293	*CTR9*	0.063	-	*NCLN*	0.259	-
EFNA3	0.133	-	*PPP1R3C*	0.070	-1203	*GIMAP1*	0.266	-
ETV5	0.152	-	*STEAP2*	0.075	-	*LHFPL5*	0.286	-720
GSTA4	0.156	-	*FRY*	0.079	-	*ADARB1*	0.345	-17
TRPM7	0.159	-	*LOC441124*	0.080	-	*SRGAP1*	0.450	-105
ADM	0.177	-155/-720	*APC*	0.086	-17/-155	*KCTD15*	0.471	-720
FGD2	0.181	-	*MMP28*	0.087	-	*MATR3*	0.482	-
SMAD7	0.187	-17/-720/-1289	*PDE7B*	0.093	-	*SSFA2*	0.486	-
ZNF792	0.196	-	*RUNX1T1*	0.095	-	*IFT81*	0.489	-28-5p
IPO5	0.207	-	*ANKRD10*	0.096	-	*KAAG1*	0.492	-
SPRY2	0.210	-	*HIC1*	0.107	-	*DLL4*	0.537	-
RNASEH2C	0.210	-	*C5orf4*	0.109	-720	*CBX3*	0.574	-1265
HOXA3	0.226	-	*ZNF395*	0.110	-	*FAM134B*	0.579	-
PRDX2	0.230	-	*LCORL*	0.111	-155	*WWOX*	0.582	-29a/-29b
ID1	0.255	-	*MUM1*	0.111	-	*BMP2K*	0.590	-
HDAC5	0.260	-	*KRAS*	0.116	-17/-29b/-105/-155	*FAM73A*	0.591	-105
ZNF503	0.263	-	*ALX1*	0.117	-	*AP4E1*	0.608	-1263
RECQL5	0.268	-	*ZNF792*	0.122	-	*TMEM88*	0.611	-
MYLIP	0.269	-17/-105	*SETDB2*	0.122	-	*NUDCD1*	0.628	-
FANCF	0.269	-155	*SATB1*	0.125	-191	*PHF14*	0.639	-
UBOX5	0.269	-504/-761	*LOC158376*	0.126	-	*LY6K*	0.664	-
CCDC64	0.272	-	*EBF3*	0.128	-	*CDH6*	0.668	-155/-425/-1265
KRAS	0.276	-17/-29b/-105/-155	*SPIN4*	0.133	-155	*ELF5*	0.682	-
DBT	0.276	-17/-767/-29/-4293	*SOX13*	0.133	-	*DDX24*	0.752	-
ZNF625	0.277	-	*CAPNS2*	0.134	-	*PCDHGB6*	0.765	-
FAM131A	0.283	-	*ANKRD28*	0.137	-17	*SCLY*	0.769	-
GLDN	0.285	-	*CALCRL*	0.138	-	*EXOC5*	0.771	-155/-425/-767/-761
EMP1	0.291	-	*HOXA10*	0.139	-17/-29a/-29b/-155	*RCOR1*	0.774	-155/-3169
TXNIP	0.295	-17	*DACH1*	0.140	-	*CCL21*	0.774	-
C5orf4	0.296	-720	*FAM124B*	0.141	-	*ZNF501*	0.776	-
HOXA9	0.296	-17/-155	*PTEN*	0.142	-17/-29a/-29b/-378	*FAM179B*	0.780	-
MGST1	0.298	-	*PRICKLE1*	0.142	-	*METT10D*	0.783	-
ZNF77	0.301	-155	*ID1*	0.143	-	*HIST1H3I*	0.797	-
LOC284023	0.303	-	*LOC284023*	0.146	-	*RPL10L*	0.803	-
FAM87A	0.304	-	*FBXO32*	0.147	-	*C6orf115*	0.803	-
RBM15	0.306	-	*FGD4*	0.151	-17	*C7orf30*	0.816	-
VASH1	0.309	-761/-3169	*HOXA5*	0.153	-	*SLC16A3*	0.839	-155
XPO7	0.313	-	*SAMD13*	0.153	-	*STK32C*	0.849	-
ASPH	0.323	-767-3p/-29b	*MST1*	0.154	-	*SLC25A38*	0.879	-
TTC3	0.325	-105/-720	*MYLIP*	0.155	-17/-105	*POLR2B*	0.882	-
PDIK1L	0.331	-29a	*ATF7IP2*	0.159	-	*C14orf86*	0.889	-
SNX11	0.339	-17/-761	*ZDHHC21*	0.159	-	*LARP4*	0.893	-1265
FBXO32	0.348	-	*XYLT1*	0.160	-761	*TOX*	0.900	-
ETAA1	0.348	-	*FAM84B*	0.165	-761	*MAN1A2*	0.913	-
CNDP2	0.353	-	*C16orf53*	0.165	-	*CPSF2*	0.935	
SLC5A5	0.355	-504	*ZNF248*	0.166	-	*SERINC3*	0.939	-
RBM24	0.361	-	*NOS3*	0.166	-155	*PPIL2*	0.949	-
PLAG1	0.367	-155	*GATA3*	0.167	-155/-720	*C10orf92*	0.955	-
PROM2	0.369	-767-5p	*MBD5*	0.169	-	*ATRIP*	0.960	-
LCE1E	0.371	-	*LIMCH1*	0.169	-105	*CLK4*	0.999	-
ZNF398	0.373	-	*PCDH17*	0.170	-504	*DNAJC12*	1.008	-
ZNF626	0.377	-155	*ZFPM1*	0.170	-	*NME6*	1.028	-
ING5	0.378	767-3p	*C21orf34*	0.175	-	*TFEC*	1.028	-29a/-29b
HOXA5	0.378	-	*STK38L*	0.177	-	*BRPF3*	1.043	-
AXIN2	0.381	767-5p	*SUZ12P*	0.177	-	*C19orf44*	1.064	-
FOXC1	0.382	-	*STYK1*	0.179	-1265	*SLC25A33*	1.081	-
ZNF786	0.382	-105	*TRIM45*	0.181	-	*KLHL22*	1.084	-
C21orf34	0.383	-	*TTLL5*	0.181	-	*TRIML2*	1.125	-
ZNF19	0.385	-	*PELI2*	0.182	-	*RPL24*	1.152	-
ZNF680	0.386	-155	*PALMD*	0.182	-1265	*F11R*	1.162	-
AXL	0.386	-	*ARHGAP18*	0.183	-155	*ZNF229*	1.176	-
RAD23B	0.388	-155	*DNAJB4*	0.183	-155	*CIDEC*	1.189	-
ZNF420	0.389	-425	*SLC40A1*	0.184	-	*ZNF460*	1.192	-
ZNF564	0.389	-	*ZBTB20*	0.187	-761	*RHOU*	1.234	-767-3p
CALU	0.389	-	*FAT4*	0.187	-	*GAPDH*	1.246	-29a/-155
ZFP3	0.393	-17	*GFOD1*	0.188	-	*CTTNBP2NL*	1.249	-29a/-29b
PNPLA3	0.394	-28-3p	*SLC2A12*	0.188	-767-3p/-155	*ASAP1*	1.254	-
CBR4	0.394	-	*SNAP91*	0.189	-1263	*ANO1*	1.261	-
C15orf42	0.394	-	*PHACTR2*	0.190	-767-3p/-155	*TMEM132D*	1.295	-425
FZD8	0.395	-	*GSK3A*	0.192	-	*DHX9*	1.312	-
ID3	0.396	-29b/-155	*ST8SIA4*	0.192	-1263	*BAG1*	1.379	-28-5p
ZMYM2	0.396	-155	*NHLRC3*	0.193	-28-3p	*ANKS1B*	1.400	-
GATA3	0.402	-155/-720	*ZNF625*	0.194	-	*CDC2L2*	1.597	-
PTCRA	0.406	-	*ABHD6*	0.195	-	*NRIP1*	1.627	-
PURG	0.407	-29a/-29b	*PCDH7*	0.195	-761	*TBCD*	1.644	-
NSUN3	0.409	-	*MTUS1*	0.196	-4293	*SYNM*	1.659	-
FAM84B	0.410	-761	*THSD1*	0.198	-	*CARD18*	1.659	-
NUCKS1	0.410	-	*ACOX2*	0.198	-	*COX6A1*	1.714	-
FGD6	0.411	-761/-720	*ACVR1B*	0.199	-761/-720	*RGMA*	1.726	-17
ZNF228	0.411	-	*GNAI1*	0.199	-	*CCDC42*	1.753	-
EIF2C1	0.412	-28-5p/-105/-155/-761	*MGC24039*	0.199	-720	*TANC2*	1.952	-767-3p/-4293
PAPD4	0.412	-	*CSMD1*	0.200	-155/-4293	*GABRD*	2.000	-
NBPF1	0.412	-	*KLF15*	0.200	-1265	*MAPT*	2.016	-767-3p
ARID4A	0.414	-17/-3169	*TXNRD2*	0.201	-17	*FOXL2*	2.089	-17
ATAD3B	0.415	-155	*HOXA9*	0.203	-17/-155	*IL1RAPL2*	3.373	-
SLC35D2	0.416	-	*RPS6KA5*	0.203	-17	*PARP15*	3.500	-
ZNF397	0.417	-	*PROM2*	0.203	767-5p	*CD1E*	3.538	-
LRP6	0.418	-29a/-29b	*GPAM*	0.205	-105/-155	*KLHL31*	3.968	-
CHD1L	0.418	-4293	*C18orf54*	0.205	-	*UNC5B*	4.368	-
ID2	0.419	-	*THBD*	0.205	-	*JPH2*	6.836	-761
LYSMD1	0.421	-29a/-29b	*FGD2*	0.205	-	*TLE6*	8.222	-
ZKSCAN5	0.421	-	*CYYR1*	0.207	425	*ABCC9*	8.611	-155
TRAM2	0.424	-720	*ZNF682*	0.208	-	*GLT8D4*	9.554	-
HIC1	0.424	-	*FLJ41603*	0.211		*FGF18*	11.955	-

Supplementary Table S5. Properties of *SAMD4A* and *EXT1* genic contacts detected by ChIA-PET.

SAMD4A

0 min contacts

gene	PETs	chr	array	ChIP-seq p65	ChIP-seq polII
CGRRF1	17	14			
GCH1	12	14			
•*WDHD1*	8	14			
CNIH	5	14			
GMFB	5	14			
CDKN3	4	14			
•*SOCS4*	4	14			
FBXO34	3	14			
FERMT2	3	14			
•*FLRT2*	3	14			
•*FRMD6*	3	14			
•*LTBP2*	3	14			
•*PSMA3*	3	14			

30 min contacts

gene	PETs	chr	array	ChIP-seq p65	ChIP-seq polII
CGRRF1	80	14			
GCH1	30	14			
GMFB	23	14			
WDHD1	20	14			
CNIH	11	14			
CDKN3	8	14			
DDAH1	6	1			
PTPRK	6	6			
TANK	6	2			
FERMT2	5	14			
SOCS4	5	14			
APP	4	21			
DPF3	4	14			
EXOC6	4	10			
FNDC3B	4	3			
FRMD6	4	14			
GRID2	4	4			
HRH1	4	3			
ITGAV	4	2			
LPIN1	4	2			
MAPK1IP1L	4	14			
MAST4	4	5			
MYOF	4	10			
RAD51L1	4	14			
SMAD3	4	15			
SVIL	4	10			
TCF12	4	15			
ANKRD28	3	3			
ANO2	3	12			
CALD1	3	7			
CDC73	3	1			
CDH5	3	16			
CDK17	3	12			
COL4A1	3	13			
COL4A2	3	13			
CSMD1	3	8			
CTNNA3	3	10			
DLGAP5	3	10			
DMD	3	X			
ERBB4	3	2			
ETV6	3	12			
FILIP1	3	6			
FRMD4B	3	3			
GIMAP8	3	7			
HSPG2	3	1			
KDM6A	3	X			
KLF7	3	2			
MBNL2	3	13			
MCTP1	3	5			
MYO5A	3	15			
NAV2	3	11			
NEDD9	3	6			
PARK2	3	6			
PODXL	3	7			
PPFIBP1	3	12			
RALA	3	7			
RBMS3	3	3			
SGK1	3	6			
SLC39A11	3	17			
SPOCK1	3	5			
SQSTM1	3	5			
TCF4	3	18			
TMEM132C	3	12			
TRAF1	3	9			
TTC7B	3	14			
ZEB1	3	10			
ZFPM2	3	8			
ZNF407	3	18			

EXT1

0 min contacts

gene	PETs	chr	array	ChIP-seq p65	ChIP-seq polII
•*SAMD12*	98	8			
NCRNA00252	6	8			
MED30	5	8			
•*ZFPM2*	3	8			
•*CDH5*	3	16			
•*HSPG2*	3	1			

30 min contacts

gene	PETs	chr	array	ChIP-seq p65	ChIP-seq polII
SAMD12	333	8			
NCRNA00252	18	8			
MED30	11	8			
EIF3H	8	8			
TNFRSF11B	4	8			
DOCK4	4	7			
FNDC3B	4	3			
GPR56	4	16			
ASAP2	3	2			
COLEC10	3	8			
EIF2C2	3	8			
NSE2	3	8			
ADAMTS9	3	3			
CTNNA1	3	5			
DDAH1	3	1			
EGFL7	3	9			
ETS1	3	11			
EXOC6	3	10			
MACF1	3	1			
MEF2A	3	15			
PARK2	3	6			
PTPRB	3	12			
RANBP17	3	5			
RASA1	3	5			
RPS6KA2	3	10			
SCFD2	3	4			
TCF4	3	18			
ZFP36	3	19			

Supplementary Table S6. Properties of genic contacts made by genes hosting miR-17, -155, and -191 (detected by ChIA-PET).

MIR17HG

chr	hits	gene name	hosted miRNA	array	ChIP-seq p65	ChIP-seq polII
13	3	GPC5				
13	3	GPC6				
10	2	FRMD4A	mir-4293/-1265			
13	1	A2LD1				
13	1	ABHD13				
2	1	BCL2L11				
12	1	C12orf70				
X	1	CAPN6				
16	1	CLEC16A				
6	1	CNKSR3				
16	1	CNOT1				
10	1	CTBP2	mir-4296			
13	1	DNAJC3				
3	1	FSTL1	mir-98			
5	1	GPBP1				
17	1	KCNH4				
8	1	KCNQ3				
13	1	LMO7				
6	1	MTHFD1L				
3	1	NLGN1				
11	1	PICALM				
19	1	PRKD2	mir-320e			
13	1	RBM26				
21	1	RCAN1				
20	1	RIN2				
10	1	STAM				
1	1	TMEM51				
10	1	ZNF518A				

MIR155HG

chr	hits	gene name	hosted miRNA	array	ChIP-seq p65	ChIP-seq polII
21	20	MRPL39				
21	20	NCRNA00158	NCRNA00158			
21	12	JAM2				
21	9	APP				
21	4	BACH1	NCRNA00189			
21	3	ATP5J				
3	2	ADAMTS9				
5	2	DDX46				
10	2	EXOC6				
21	2	GABPA				
21	2	GRIK1	NCRNA00258			
21	2	HSPA13				
7	2	LOC646329	mir-29a/-29b1			
15	2	MEX3B				
17	2	MYH10				
19	2	PCSK5				
1	2	SELE				
14	2	TNFAIP2				
6	2	USP45				
1	2	VCAM1				
16	1	ACD				
9	1	ACO1				
21	1	ADAMTS1				
1	1	ADORA1				
19	1	AKT2	mir-641			
11	1	AMBRA1	mir-3160-1/-2			
17	1	ANKRD13B				
17	1	AP2B1				
2	1	ARHGAP15				
2	1	ARHGAP25				
2	1	ARPC2				
6	1	ATXN1				
17	1	BCAS3				
12	1	BCAT1				
10	1	C10orf53				
14	1	C14orf147				
21	1	C21orf34	mir-99a/-125b2/let-7c			
21	1	C21orf7				
21	1	C21orf91	NCRNA00157			
5	1	C6				
6	1	C6orf99				
1	1	CASZ1				
14	1	CDC42BPB				
5	1	CDC42SE2				
16	1	CDH11				
20	1	CDH22				
10	1	CDH23				
6	1	CDYL				
7	1	CFTR				
21	1	CHODL				
13	1	COL4A2				
16	1	CPPED1	mir-4718			
17	1	CRHR1				
17	1	CSNK1D				
11	1	CTTN				
21	1	CXADR				
5	1	DCP2				
3	1	DGKG				
10	1	NCRNA00093	NCRNA00093			
2	1	DOCK10				
1	1	ELTD1				
22	1	ENTHD1				
14	1	ESRRB				
14	1	EXOC3L4				
4	1	EXOSC9				
9	1	FAM154A				
10	1	FAM171A1				
18	1	FAM38B				
6	1	FARS2				
14	1	FRMD6				
16	1	FUK				
6	1	FYN				
12	1	GABARAPL1				
X	1	GNL3L				
9	1	GPSM1				
2	1	HAT1				
2	1	HEATR5B				
1	1	IFFO2	mir-1290			
7	1	IGF2BP3				
21	1	ITSN1				
2	1	ITSN2				
8	1	JRK				
1	1	KCND3				
21	1	KCNJ6				
12	1	KRAS2				
17	1	KSR1				
21	1	LCA5L				
4	1	LCORL				
3	1	LOC100507391	LOC100507391			
2	1	LOC284998	LOC284998			
10	1	LOC728558	mir-3157			
11	1	LRP5				
14	1	LRRC9				
14	1	LTBP2				
21	1	LTN1				
4	1	MAML3				
X	1	MAP7D2				
14	1	MARK3				
6	1	ME1				
22	1	MIR130B/-301b	mir-130b/-301b			
19	1	MIR3190/3191	mir-3190/-3191			
1	1	MIR3658	mir-3658			
16	1	MIR4719	mir-4719			
16	1	MIR548X	mir-548x			
11	1	MIR675	mir-675			
14	1	MLH3				
6	1	MRPL14				
1	1	MTOR				
11	1	MUC5B				
17	1	MYO1D				
19	1	NACC1				
21	1	NCAM2				
2	1	NCRNA00299	NCRNA00299			
21	1	MIR3197	mir-3197			
11	1	NDUFC2-KCTD14				
14	1	NFKBIA				
17	1	NMT1				
21	1	NRIP1				
14	1	NRXN3	mir-548a3			
1	1	OBSCN				
6	1	OFCC1				
10	1	PARD3				
21	1	PDE9A				
10	1	PDLIM1				
17	1	PIK3R5				
19	1	PLEKHA4				
6	1	PLEKHG1				
12	1	PLEKHG7				
2	1	POLR1A				
2	1	POLR2D				
22	1	PPP6R2				
14	1	PRKD1				
8	1	PTDSS1				
11	1	PTPRJ	mir-3161			
22	1	RANGAP1				
15	1	RASGRP1				
4	1	RELL1				
3	1	RFTN1				
4	1	RGS12				
9	1	RGS3				
6	1	RIMS1				
X	1	RP2				
1	1	RPRD2				
3	1	RSRC1				
21	1	RUNX1				
21	1	RWDD2B				
3	1	RYBP				
5	1	SAP30L				
21	1	SCAF4				
3	1	SEMA5B				
22	1	SERPIND1				
14	1	SETD3				
4	1	SH3RF1				
17	1	SLC9A3R1				
13	1	SMAD9				
7	1	SMURF1				
10	1	CCAR1	mir-1254			
14	1	SNX6				
9	1	SPINK4				
5	1	SREK1IP1				
3	1	ST6GAL1				
7	1	STEAP1B				
10	1	TAF3				
2	1	TANC1				
4	1	TBC1D1				
22	1	TBC1D22A				
3	1	TBL1XR1				
16	1	TCF25				
6	1	NCRNA00242				
11	1	TECTA				
15	1	THSD4				
21	1	TMPRSS15				
6	1	TNFAIP3				
17	1	FAM33A	mir-301a/-454			
1	1	UBR4				
10	1	UPF2				
21	1	URB1				
21	1	USP25				
2	1	USP34				
3	1	VPS8				
6	1	VTA1				
17	1	WBP2				
16	1	WDR59				
22	1	XBP1				
18	1	YES1				
3	1	ZBTB38				
10	1	ZEB1				
19	1	ZNF430				
19	1	ZNF559				

DALRD3

chr	hits	gene name	hosted miRNA	array	ChIP-seq p65	ChIP-seq polII
3	5	QRICH1				
3	4	ARIH2				
3	3	USP19				
3	2	IHPK2				
3	2	PRKAR2A				
15	1	ADAMTS17				
1	1	ADCY10				
3	1	ASB14				
3	1	BSN				
11	1	C11orf52				
3	1	MIR3137	mir-3137			
15	1	MYO1E	mir-2116			
5	1	CCNH				
3	1	CDC25A				
3	1	CELSR3				
13	1	CLDN10				
3	1	EXOSC7				
13	1	DACH1				
5	1	EGR1				
3	1	FLNB				
1	1	GPATCH4				
19	1	HIF3A				
3	1	ISY1				
16	1	ITGAL				
3	1	KLHDC8B				
6	1	LACE1				
10	1	LOC100216001	LOC100216001			
17	1	MAPT				
15	1	MYEF2				
4	1	OTUD4				
11	1	P4HA3				
4	1	PCGF3				
4	1	PDS5A				
1	1	PLXNA2				
10	1	RAB18				
5	1	RHOBTB3				
14	1	RHOJ				
14	1	RNF31				
1	1	S1PR1				
15	1	SMAD3				
3	1	SMARCC1				
22	1	SMTN				
17	1	SMURF2				
7	1	TECPR1				
3	1	TFDP2				
X	1	TSPAN6				
22	1	MIR3199-1/-2	mir-3199-1/-2			
3	1	USP4	mir-4271			
13	1	XPO4				
8	1	ZHX2				
10	1	PCDH15	mir-548f1			

Supplementary Table S7. Some genic contacts seen in 4C libraries (prepared using *SAMD4A* and *EXT1* as reference points) are TGFβ-responsive.

***SAMD4A* contacts**					***EXT1* contacts**					**random set**			
			TNFα	TGFβ				TNFα	TGFβ			TNFα	TGFβ
gene	**chr**	**hits**	**response**	**response**	**gene**	**chr**	**hits**	**response**	**response**	**gene**	**chr**	**response**	**response**
FBXO34	14	8			*JAKMIP2*	5	9			*ABCC9*	12		
TNFAIP2	14	8			*DAGLA*	11	8			*ADARB1*	21		
C10orf12	10	7			*FGGY*	1	8			*ANKS1B*	12		
FERMT2	14	7			*SAMD12*	8	8			*ANO1*	11		
IL4R	16	7			*C2orf55*	2	7			*BAG1*	9		
LARP1B	4	7			*DARS*	2	7			*BMP2K*	4		
AP4S1	14	6			*DOCK11*	X	7			*CARD18*	11		
ARHGAP5	14	6			*KIF21A*	12	7			*CBX3*	7		
CCNF	16	6			*NUP153*	6	7			*CCDC42*	17		
FRMD6	14	6			*SLC30A8*	8	7			*CIDEC*	3		
GCH1	14	6			*BAGE*	21	6			*CLK4*	5		
PRKCA	17	6			*CCDC54*	3	6			*CPSF2*	14		
ATP8A2	13	5			*CHRDL1*	X	6			*DDX24*	14		
MYH9	22	5			*CLEC2D*	12	6			*DLL4*	15		
PRKD1	14	5			*DDX60*	4	6			*ELF5*	11		
SLC6A5	11	5			*FLJ21511*	4	6			*ESR1*	6		
AKAP6	14	4			*GRIA3*	X	6			*FAM179B*	14		
C11orf65	11	4			*ABCA9*	17	5			*FAM73A*	1		
CNIH	14	4			*DLG2*	11	5			*FGF18*	5		
GNL1	6	4			*KIF1B*	1	5			*GAPDH*	12		
KRT6B	12	4			*MYO9A*	15	5			*GIMAP1*	7		
PTRF	17	4			*CAST*	5	4			*GLT8D4*	3		
SLC39A11	17	4			*LCOR*	10	4			*HIST1H3I*	6		
ZNF608	5	4			*RNF43*	17	4			*IFT81*	12		
ACCN1	17	3			*RPAP3*	12	4			*IL1RAPL2*	X		
C14orf43	14	3			*TGFA*	2	4			*LATS2*	13		
C14orf50	14	3			*YT521*	4	4			*LHFPL5*	6		
C14orf70	14	3			*ZNF704*	8	4			*DHX9*	1		
CGRRF1	14	3			*LRIG3*	12	3			*LRRC7*	1		
CITED2	6	3			*LRRTM4*	2	3			*MAN1A2*	1		
DDHD1	14	3			*MED30*	8	3			*MATR3*	5		
KLF12	13	3			*OAS2*	12	3			*METT10D*	17		
LIN52	14	3			*RGS22*	8	3			*MIR15A*	13		
LRRIQ1	12	3			*TPTE*	21	3			*NCLN*	19		
SNX24	5	3			*TTC21B*	10	3			*NRIP1*	21		
TMCC3	12	3			*C10orf76*	10	2			*NUDCD1*	8		
BRMS1L	14	3			*CHST11*	12	2			*PAK3*	X		
ZNF267	16	3			*DCTN6*	8	2			*PARP15*	3		
ABCA3	16	2			*KCNAB1*	3	2			*PHF14*	7		
ARHGEF17	11	2			*PIGW*	17	2			*POLR2B*	4		
CALR3	19	2			*RBPMS*	8	2			*RCOR1*	14		
CDKN3	14	2			*RELN*	7	2			*RGMA*	15		
EFTUD2	17	2			*RIMS2*	8	2			*RHOU*	1		
FAM179B	14	2			*RIT1*	1	2			*SSFA2*	2		
PSMC1	14	2			*TLL1*	4	2			*SLC16A3*	17		
SPAG16	2	2			*RNLS*	10	2			*SSTR1*	14		
STRN3	14	2			*RPS6KA2*	6	2			*STYK1*	12		
TM9SF2	13	2			*MATR3*	5	2			*TANC2*	17		
BCKDHB	6	2			*NDST4*	4	2			*TOX*	8		
ENC1	5	2			*XIAP*	X	2			*TRIML2*	4		
ZFHX2	14	2			*WSB1*	17	2			*WWOX*	16		
VEZF1	17	2			*NSE2*	8	1			*ZNF229*	19		
PRTFDC1	10	1								*ZNF460*	19		